Calorimetry in Particle Physics

Lecture II

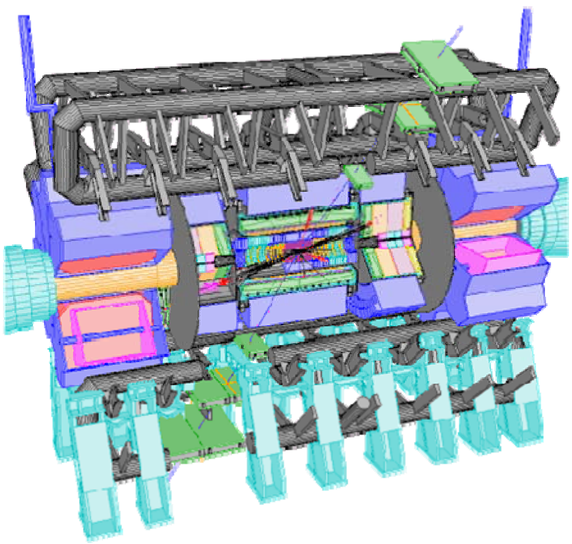

H. Oberlack
MPI für Physik, Munich

OUTLINE - 1 -

I. Overview of Calorimetry
   1. Calorimetry in Thermodynamics
   2. Nuclear Radiation Detectors
   3. Calorimetry in Particle Physics
   4. Overview of Detection Mechanisms
   5. Making of the ATLAS Lar End-caps

II. Physics of Shower Development
   1. Electromagnectic showers
   2. Muons traversing dense materials
   3. Hadronic showers
   4. Properties of the shower particles
   5. Monte Carlo simulations

III. Energy Response of Calorimeters
   1. Homogeneous calorimeters
   2. Sampling calorimeters
   3. Compensation
   4. Response of Cerenkov calorimeters

II.1 Physics of Shower Development → E.m. Showers

1. Energy loss by charged particles

2. Photon interactions
   a. Photoelectric effect
   b. Rayleigh scattering
   c. Compton scattering
   d. Pair production
   e. Photonuclear reactions

3. Electromagnetic cascades

4. Scaling variables
   a. Radiation length
   b. Molière radius

5. Electromagnetic shower profiles

6. Shower containment

II.1.1 E.m. Showers → Energy loss by charged particles

Heavy particles $M \gg m_e = m$

Bethe–Bloch formula : Mean energy loss

$$-\frac{dE}{dx} = 4\pi r_e^2 mc^2 \frac{L\cdot\rho}{A}\cdot Z\frac{z^2}{\beta^2}\left\{ln\frac{2mc^2\beta^2\gamma^2}{I} - \beta^2 - \frac{\delta}{2}\right\}$$

holds if : $\beta \cdot c > \alpha \cdot c$

no radiative effects

minimum ionizing particle (mip): $\frac{dE}{dx}$ = minimal

CORRECTIONS :

- $\beta\ c < \alpha\ c$

  Shell corrections

  $Z_{eff} < Z$ charge exchange
- nuclear recoil
- $\beta \rightarrow 1$ Fermi density effect δ

  Saturation

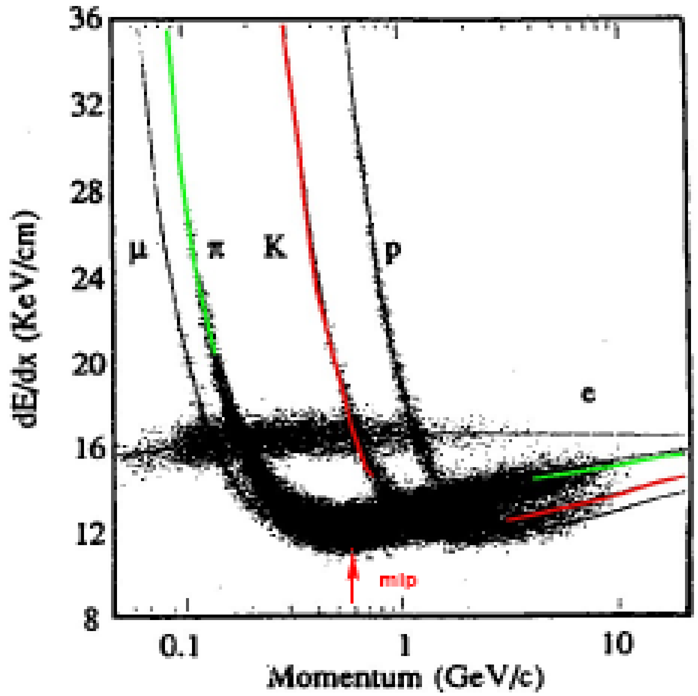

II.1.1 E.m. Showers → Energy loss by charged particles

RELATIVISTIC HEAVY PARTICLES :

Energetic knock–on electrons : δ–electrons

$$\frac{d^2N}{dT\,dx} = 2\pi r_e^2 \, \frac{L\cdot\rho}{A} \, mc^2 \, Z \, \frac{z^2}{\beta^2} \cdot \frac{1}{T^2}$$

$$T \le T_{MAX} = \frac{2mc^2 \; \beta^2 \; \gamma^2}{1+2\gamma\frac{m}{M}+(\frac{m}{M})^2}$$

High energy tail of $\frac{dE}{dx}$–distribution

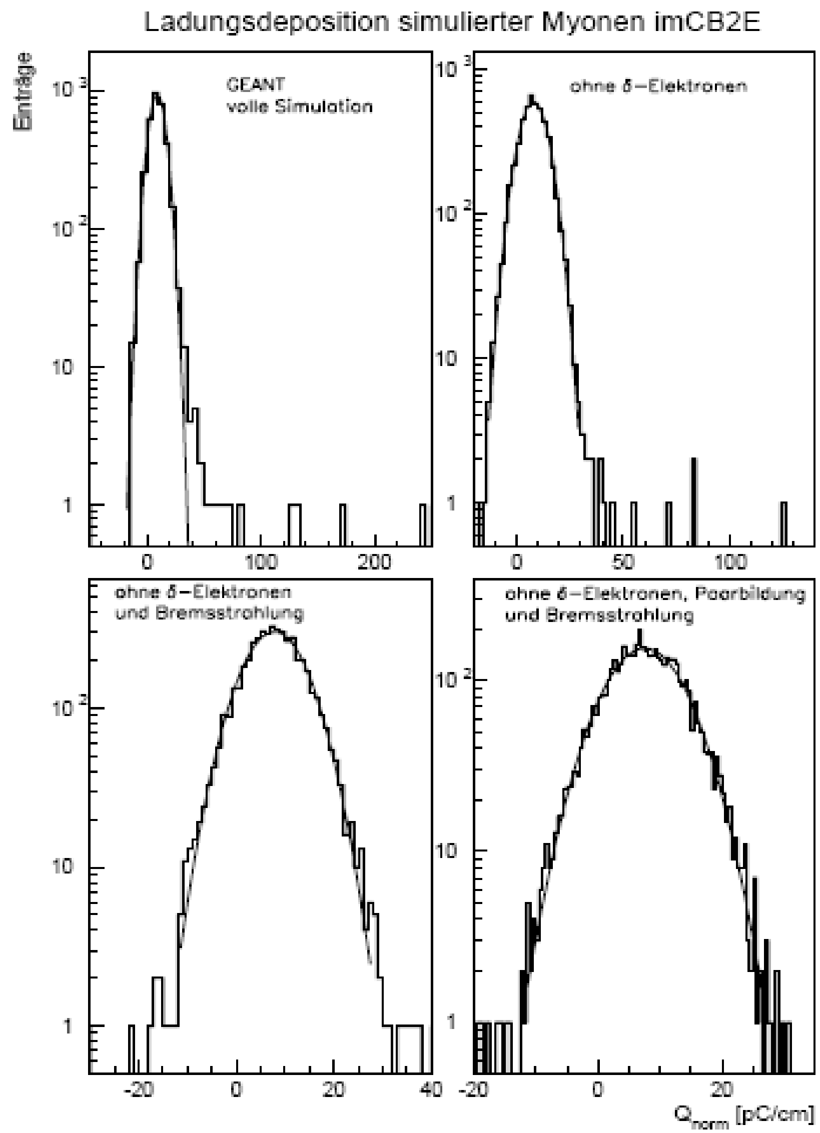

II.1.1 E.m. Showers → Energy loss by charged particles

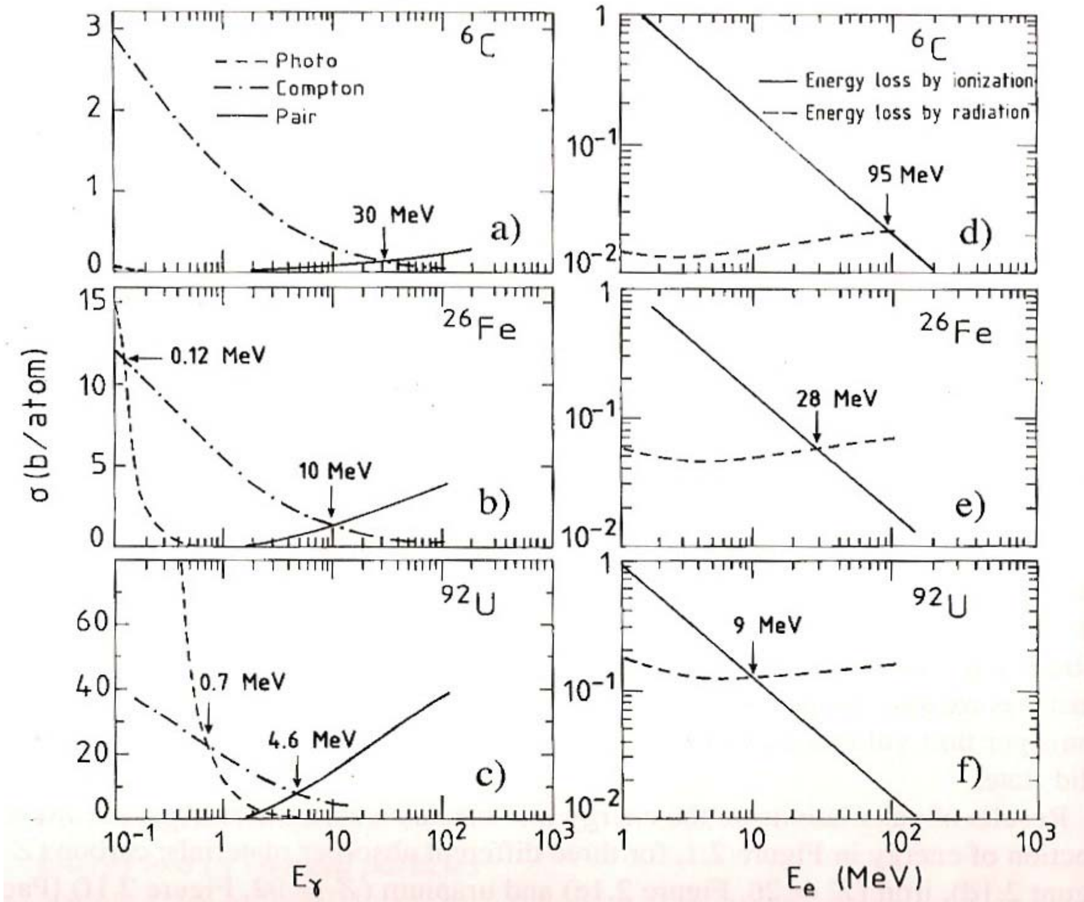

Cross sections (left) and fractional energy losses (right) through which the particles of e.m. showers lose their energy, in various absorber materials (carbon, iron, uranium).

II.1.1 E.m. Showers → Energy loss by charged particles

BREMSSTRAHLUNG

Radiation length

$$X_o = \frac{1}{4 \cdot \frac{L \cdot \rho}{A} \, Z^2 \, \frac{r_e^2}{137} \, ln \, \frac{183}{Z^{1/3}}}$$

	Scintillator	L Ar	Fe	Pb	W
$X_o[cm]$	34	14	1.76	0.56	0.35

$$\frac{d^2 w}{dx \; dE_\gamma} \approx \frac{1}{X_o} \; \frac{1}{E_\gamma}$$

$$-(\frac{dE}{dx})_\gamma \approx \frac{1}{X_o} \int_o^{E_e} E_\gamma \frac{dE_\gamma}{E_\gamma} = \frac{E_e}{X_o}$$

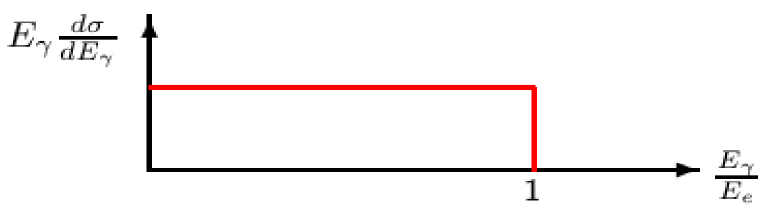

Same energy for each E_γ–interval produced.

Approximation for crude shower model :

$$< E_\gamma > = \frac{E_e}{2}$$

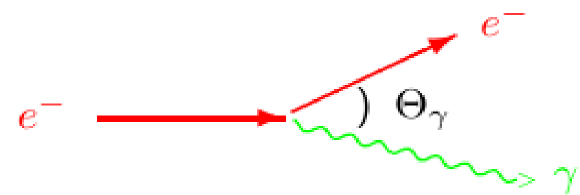

$$\sqrt{< \Theta_\gamma^2 >} = \frac{m}{E_e}$$

$$\frac{dE}{dx}|_{ion} = \frac{dE}{dx}|_{Brems} \quad \text{for} \quad E_c = \varepsilon_c$$

II.1.1 E.m. Showers → Energy loss by charged particles

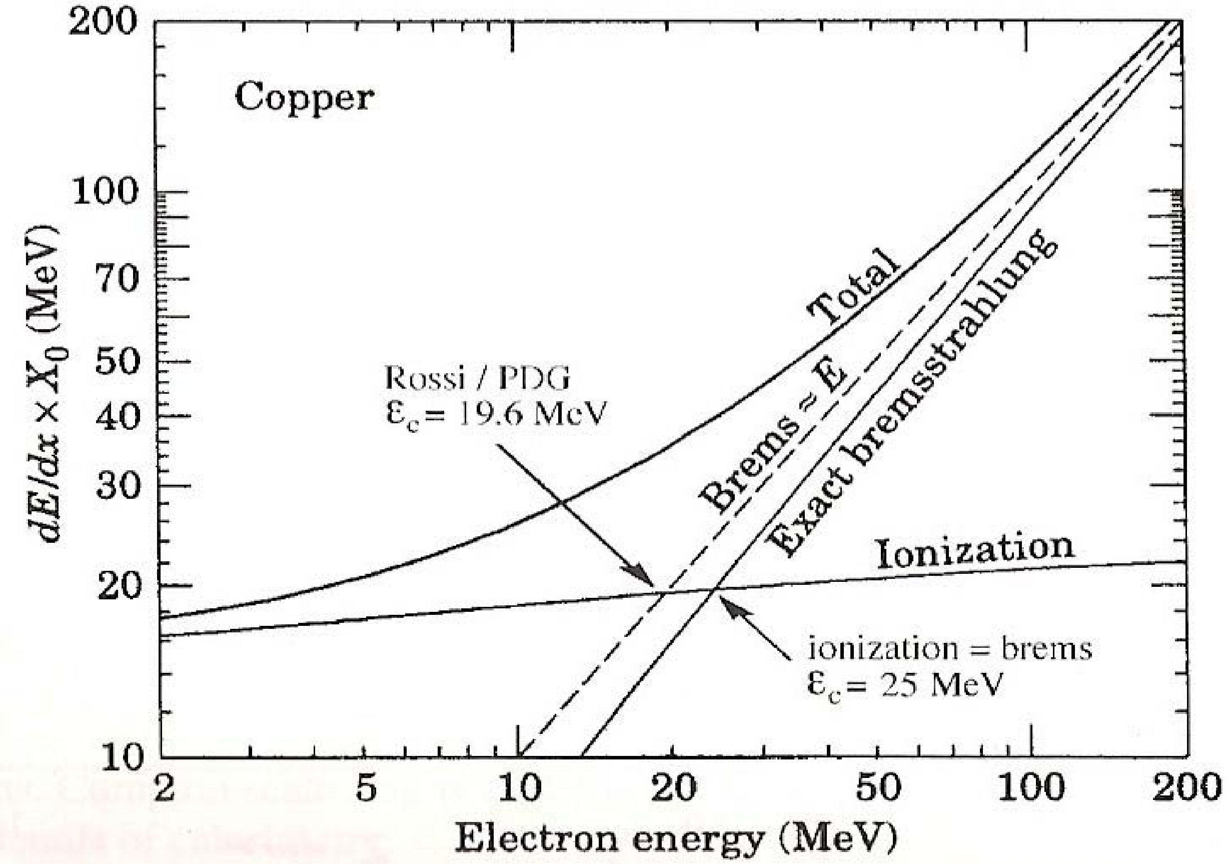

Energy losses through ionization and bremsstrahlung by electrons in copper. Arrows indicate the values for the critical energy.

II.1.2 E.m. Showers → Photon interactions

a. Photoelectric effect
b. Rayleigh scattering
c. Compton scattering
d. Pair production
e. Photonuclear reactions

II.1.1 E.m. Showers → Energy loss by charged particles

- **Interactions of Photons with Matter**

Beer's Law

$$I = I_o \; e^{- \mu \cdot x}$$

μ absorption coefficient

Photon disappears in interaction

Photoeffect

$$\gamma + A \to e^- + A^+$$

$I \ll E_\gamma \ll mc^2$

$$\sigma_{Ph} = \alpha \; \pi \; a_B^2 \; Z^5 (\frac{I_o}{E_\gamma})^{7/2}$$

$$\mu_{Ph} \sim \frac{Z^{4 \dots 5}}{E_\gamma}$$

Auger–effect $\quad A_K^+ \longrightarrow A_{L,M}^{++} + e^-$

Fluorescense radiation $\quad A_K^+ \longrightarrow A_{L,M}^+ + \gamma$

Local deposition of energy

Compton Effect

$$\gamma + e^- \to \gamma + e^-$$

$E_\gamma \to 0$ Thompson scattering

$$\sigma_{Th} = \frac{8\pi}{3} \; r_e^2 = 0.66 \; barn$$

$E_\gamma \gg mc^2 \qquad \sigma_c = \frac{3}{8} \cdot \sigma_{Th} \; \frac{mc^2}{E_\gamma} \left\{ ln \; (\frac{E_\gamma}{mc^2}) + \frac{1}{2} \right\}$

Absorption coefficient : $\quad \mu_c \sim \frac{Z}{E_\gamma}$

II.1.2 Photon interactions

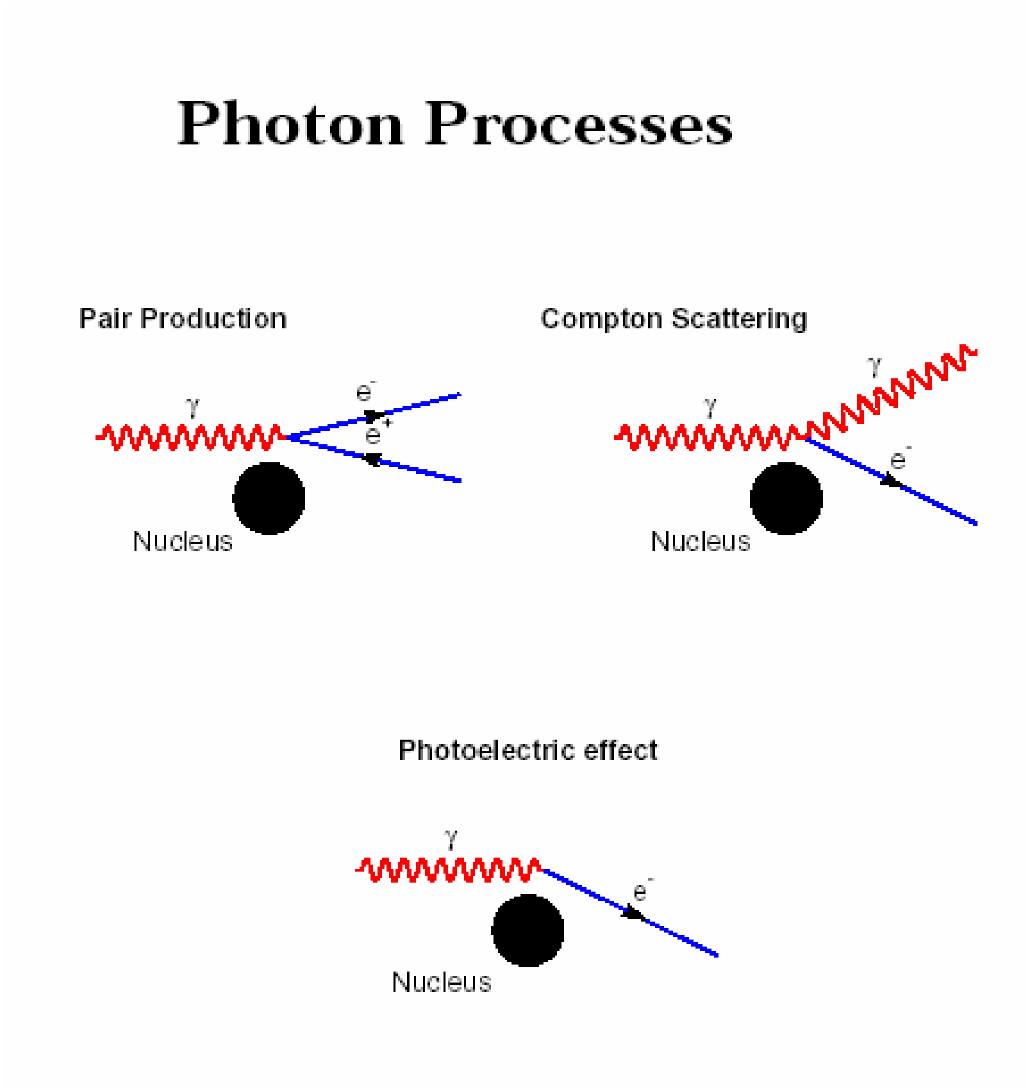

II.1.2 Photon interactions → Photoelectric effect

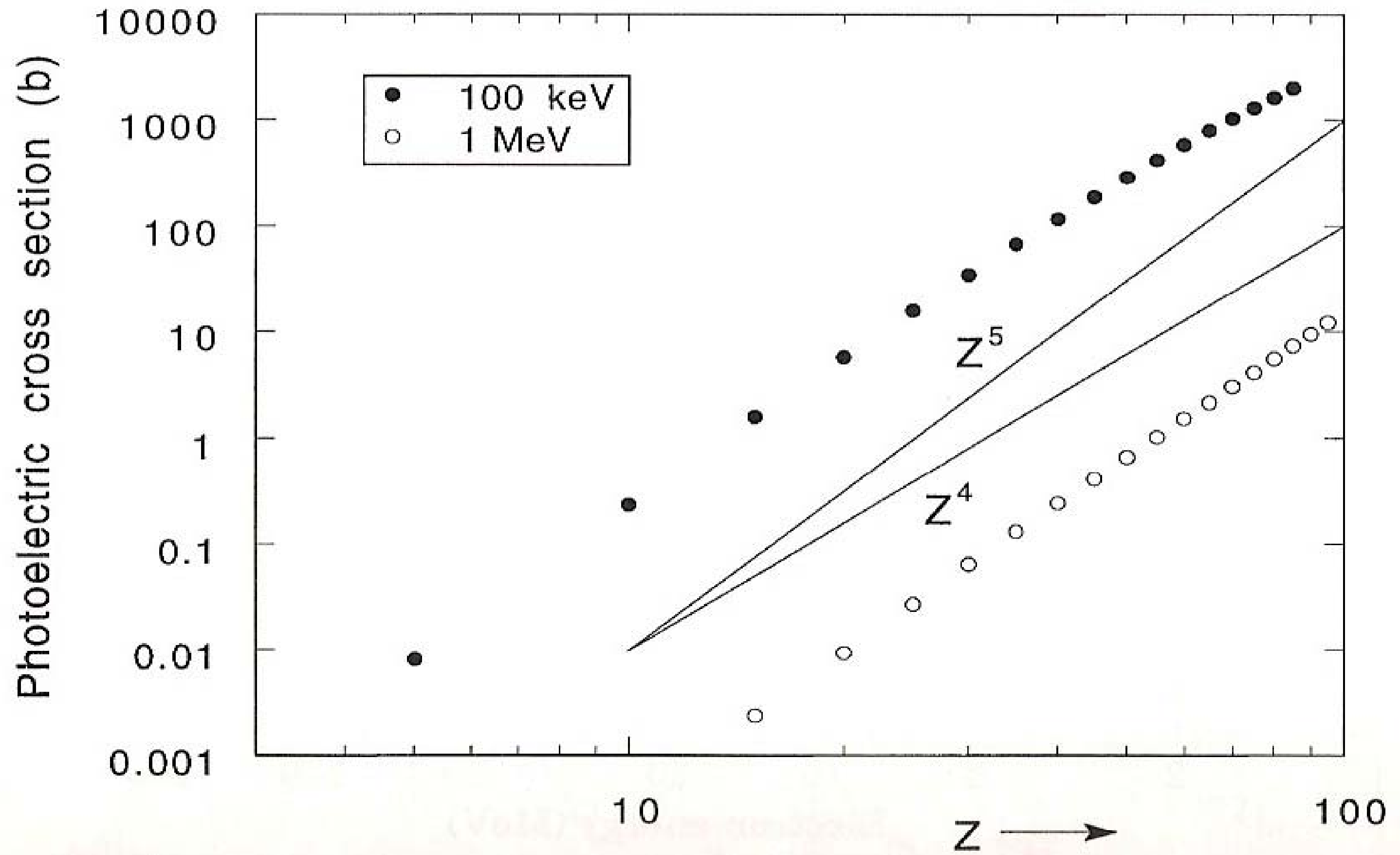

Cross section for the photoelectric effect as function of the Z value of the absorber for 100 keV and 1 MeV photons.

II.1.2 Photon interactions → Compton scattering

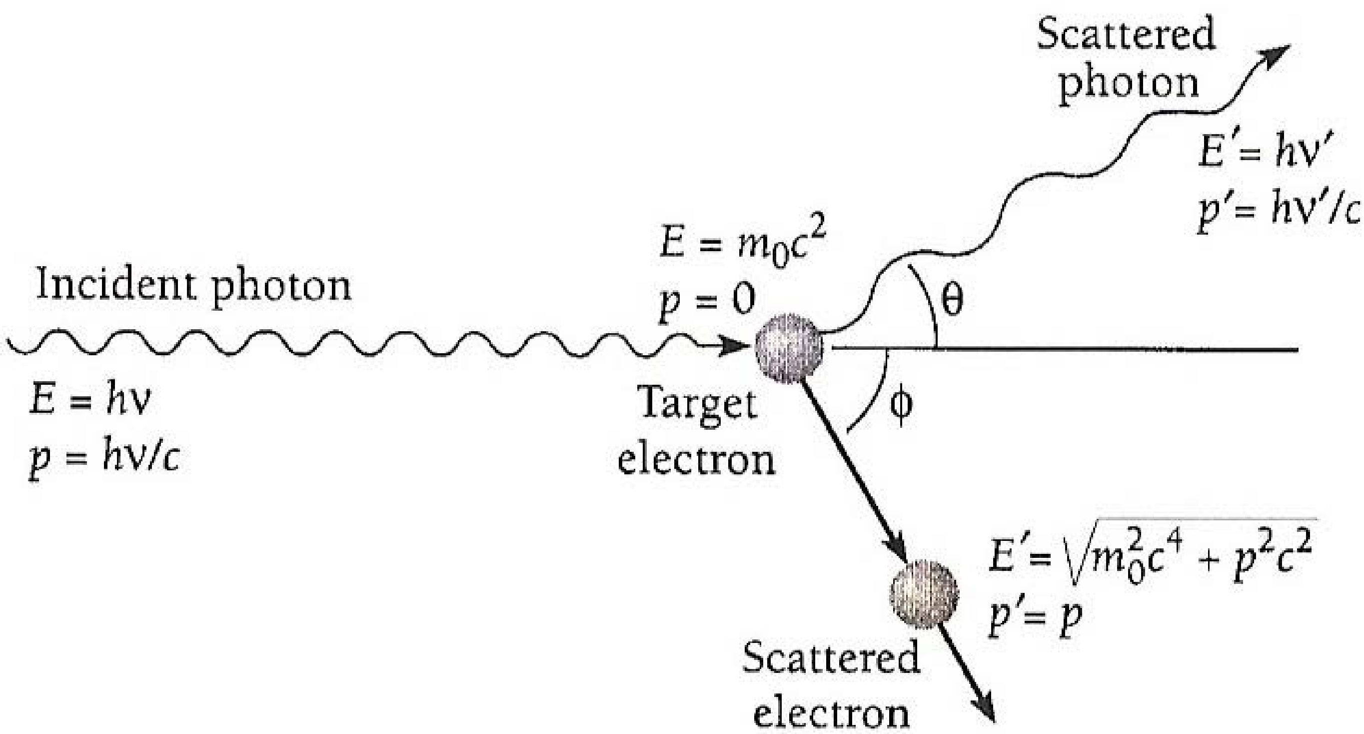

Compton scattering process

II.1.2 Photon interactions → Compton scattering

Compton Effect

$$\gamma + e^- \rightarrow \gamma + e^-$$

$E_\gamma \rightarrow 0$ Thompson scattering

$$\sigma_{Th} = \frac{8\pi}{3}\, r_e^2 = 0.66\ barn$$

$$E_\gamma \gg mc^2 \qquad \sigma_c = \tfrac{3}{8} \cdot \sigma_{Th}\, \tfrac{mc^2}{E_\gamma} \left\{ \, ln\, \left(\tfrac{E_\gamma}{mc^2}\right) + \tfrac{1}{2} \right\}$$

Absorption coefficient : $\mu_c \sim \frac{Z}{E_\gamma}$

II.1.2 Photon interactions → Compton scattering

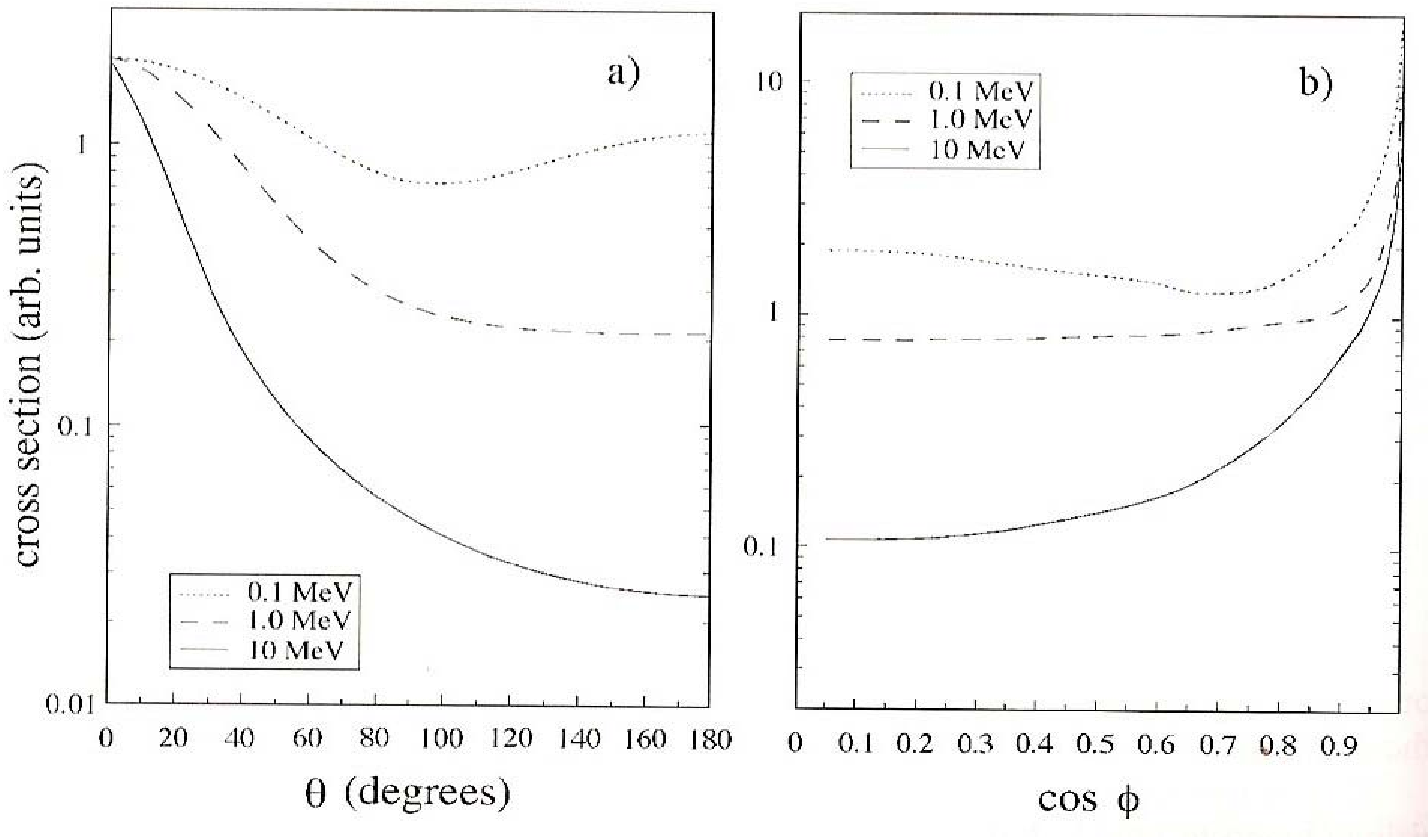

Cross section for Compton scattering as function of the scattering angle of the photon (a) and angular distribution of the Compton recoil electrons (b), for incident photons of different energies.

II.1.2 Photon interactions → Compton scattering

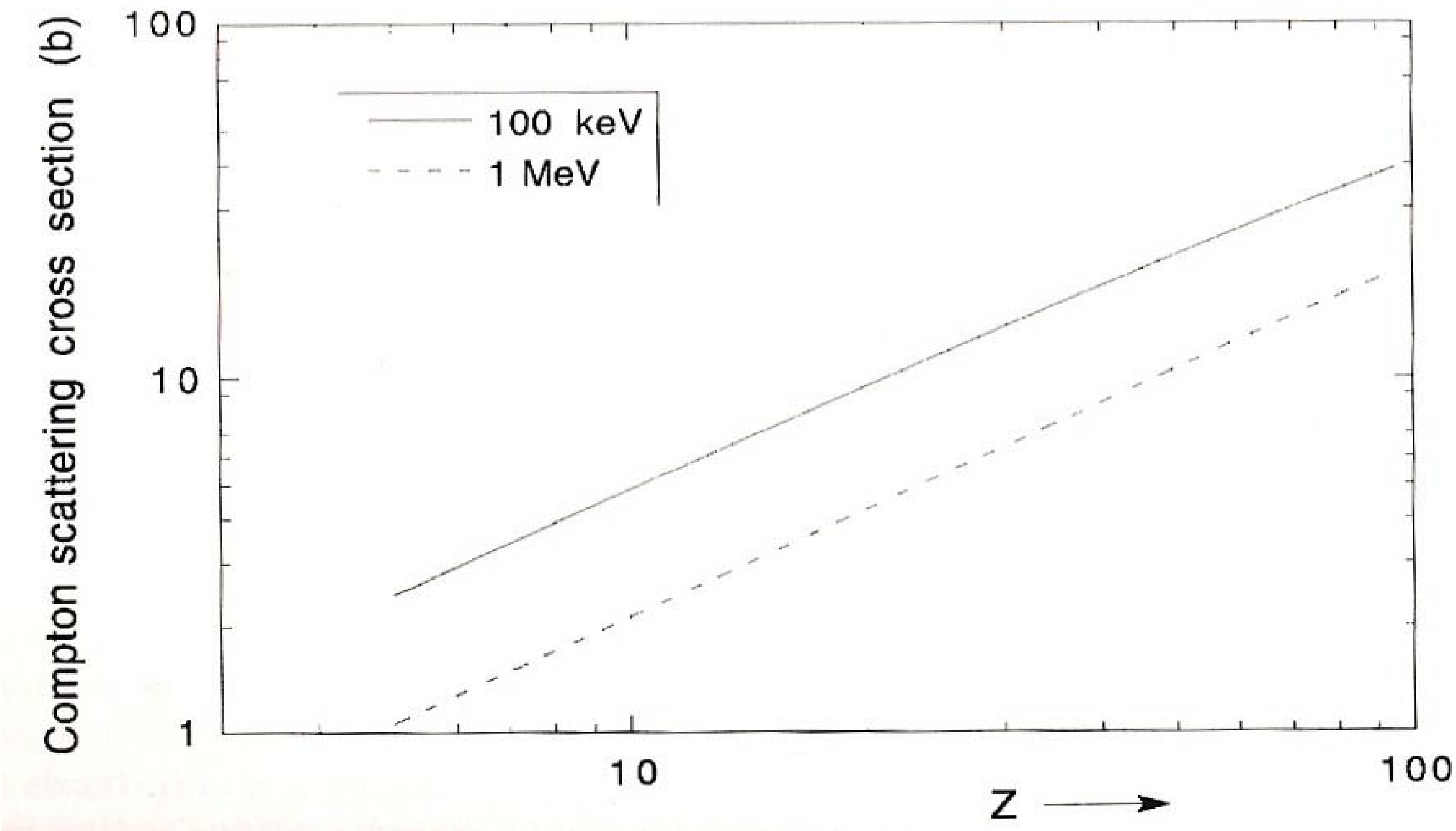

Cross section as function of the Z value of the absorber for 100 keV and 1 MeV photons.

II.1.2 Photon interactions → Pair production

PAIR PRODUCTION

$$\gamma + \text{Nucleus} \rightarrow e^+ + e^- + \text{Nucleus}$$
$$\gamma + e^- \rightarrow e^+ + e^- + e^-$$

$$\sigma_{pair} = Z^2 \, \alpha r_e^2 \left\{ \frac{28}{9} \, ln \, \frac{183}{Z^{1/3}} - \frac{2}{27} \right\}$$

Absorption coefficient

$$\mu_{pair}(E_\gamma \gg mc^2) = \frac{28}{9} \, \frac{L \cdot \rho}{A} \, Z^2 \frac{1}{137} \, r_e^2 \, ln \, \frac{183}{Z^{1/3}}$$

$$\boldsymbol{\mu_{pair} = \tfrac{7}{9} \, X_o^{-1}}$$

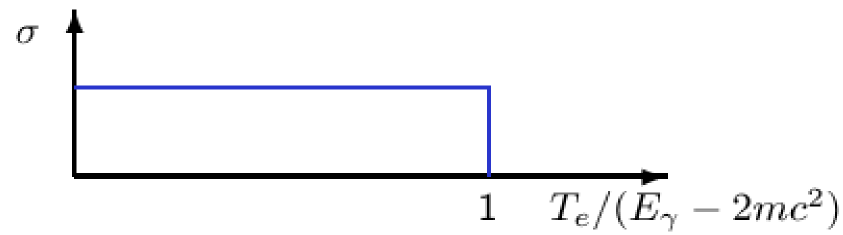

$$< \, E_\pm \, > \; \approx \; \frac{E_\gamma}{2}$$

Used as approximation in shower model

$$\sqrt{< \Theta^2 >} = \frac{mc^2}{E} = \frac{1}{\gamma}$$

Cross section for photoabsorption has a minimum

II.1.2 Photon interactions

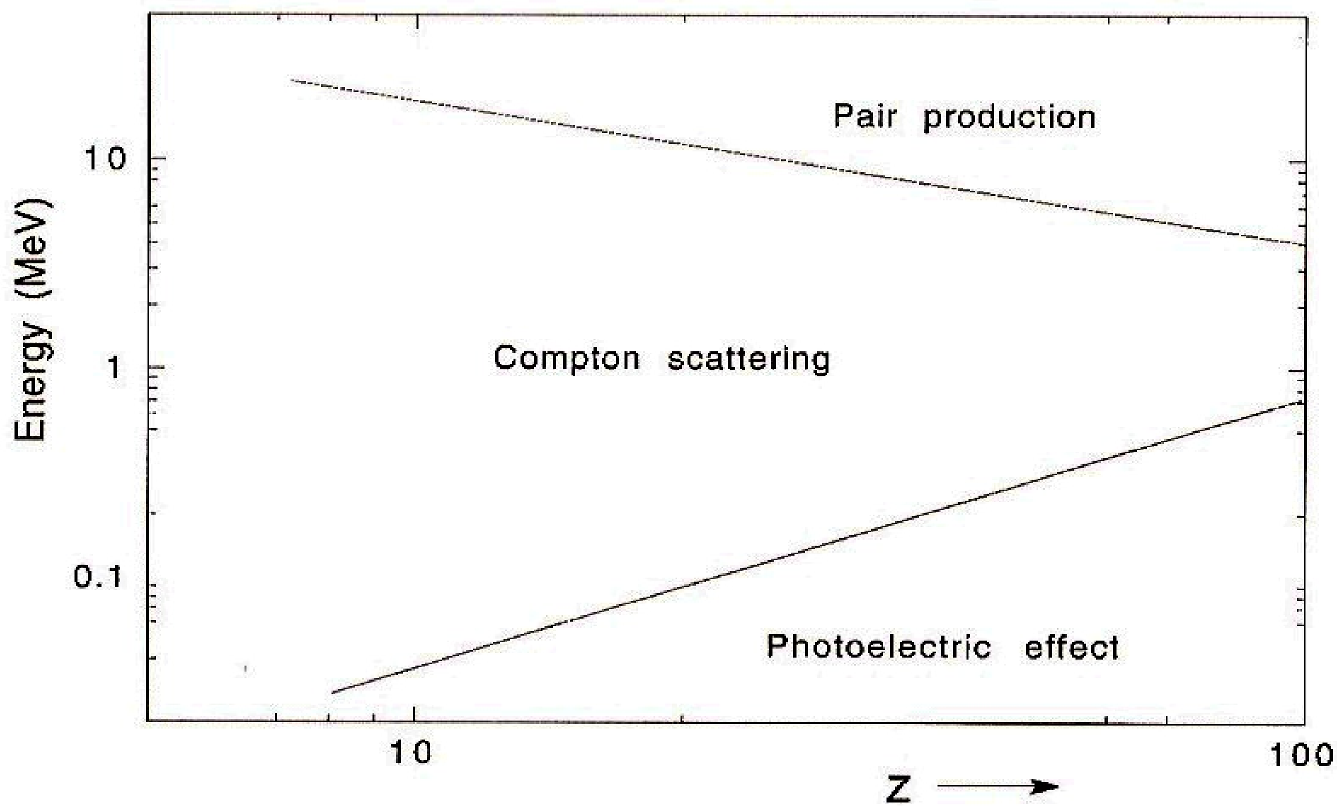

Energy domains in which photoelectric effect, Compton scattering and pair production are the most likely processes, as function of the Z value of the absorber material.

II.1.3 Electromagnetic cascades

Simple model of Heitler to discuss qualitative features

Processes considered :

$$e + Z \rightarrow e + \gamma + Z$$
$$\gamma + Z \rightarrow e^+ + e^- + Z$$

Simplifying assumptions :

- $e^\pm$ loose energy by bremsstrahlung only after $1X_o$:

$$E_\gamma = \frac{E_e}{2}$$

- After passing $1\ X_o$ of material γ materializes

$$E_\pm = \frac{E_\gamma}{2}$$

- For $E_\pm > \varepsilon_c$ energy loss due to excitation/ ionization neglected
- For $E_\pm \leq \varepsilon_c$ energy loss only due to excitation/ ionization

The longitudinal (depth) development of an electromagnetic shower

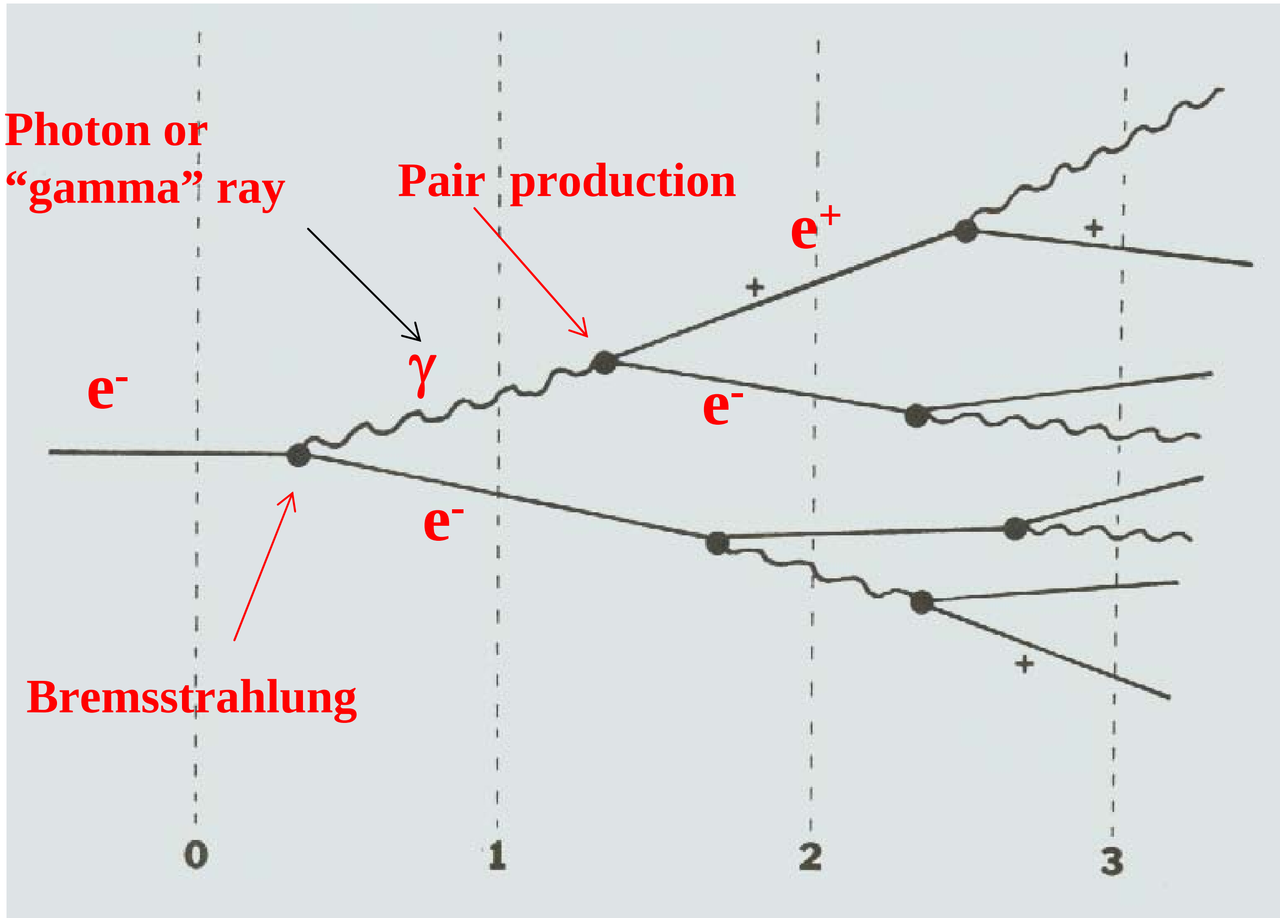

Radiation length

Number of particles

1 2 4 8 …….

II.1.3 Electromagnetic cascades

Properties of electromagnetic shower :

- number of particles in shower
- longitudinal extension of shower, position of shower maximum
- transverse dimension of shower
- transverse and longitudinal shape of shower

II.1.3 Electromagnetic cascades

- Longitudinal Extension of Shower

$$t = \frac{x}{X_o}$$

After passing thickness $t \rightsquigarrow$ number of shower particles

$$N\ (t) = 2^{\ t}$$

Energy per particle $\boldsymbol{E = \frac{E_o}{N(t)} = E_o\ 2^{-t}}$

Particles have energy ε_c after

$$t = ln\ \frac{E_o}{\varepsilon_c} / ln\ 2$$

Total number of particles with $\boldsymbol{E_1 > \varepsilon_c}$

$$N\ (E_o, E_1 > \varepsilon_c) = 2^{\ t_1} = \frac{E_o}{E_1}$$

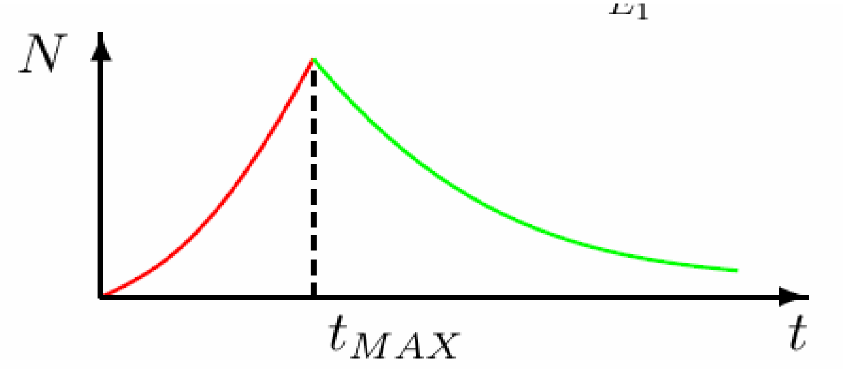

Number of particles in shower maximum :

$$\boldsymbol{N\ (E_o, \varepsilon_c) = N_{MAX} = \frac{E_o}{\varepsilon_c}}$$

Longitudinal position of shower maximum

$$\boldsymbol{t_{MAX} = ln\ E_o/\varepsilon_c}$$

Typical numbers for $E = 1$ GeV

$t_{MAX} = 3.5$

$N_{MAX} = 35$

II.1.3 Electromagnetic cascades

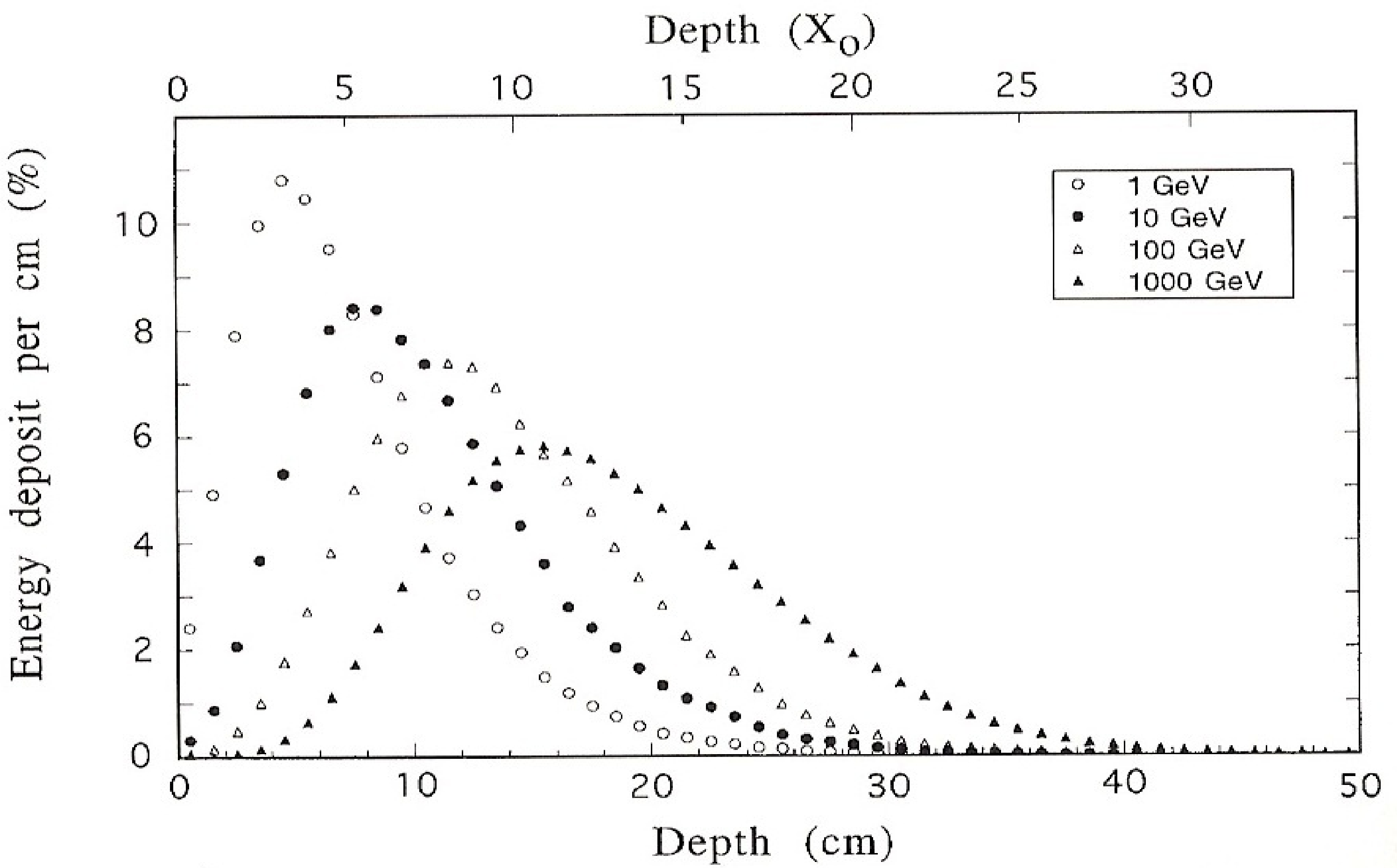

Energy deposit as function of depth for electron showers of different energy developing in a block of copper. Integrals of the curves are normalized to the same value.

Depth Development of Electromagnetic Showers

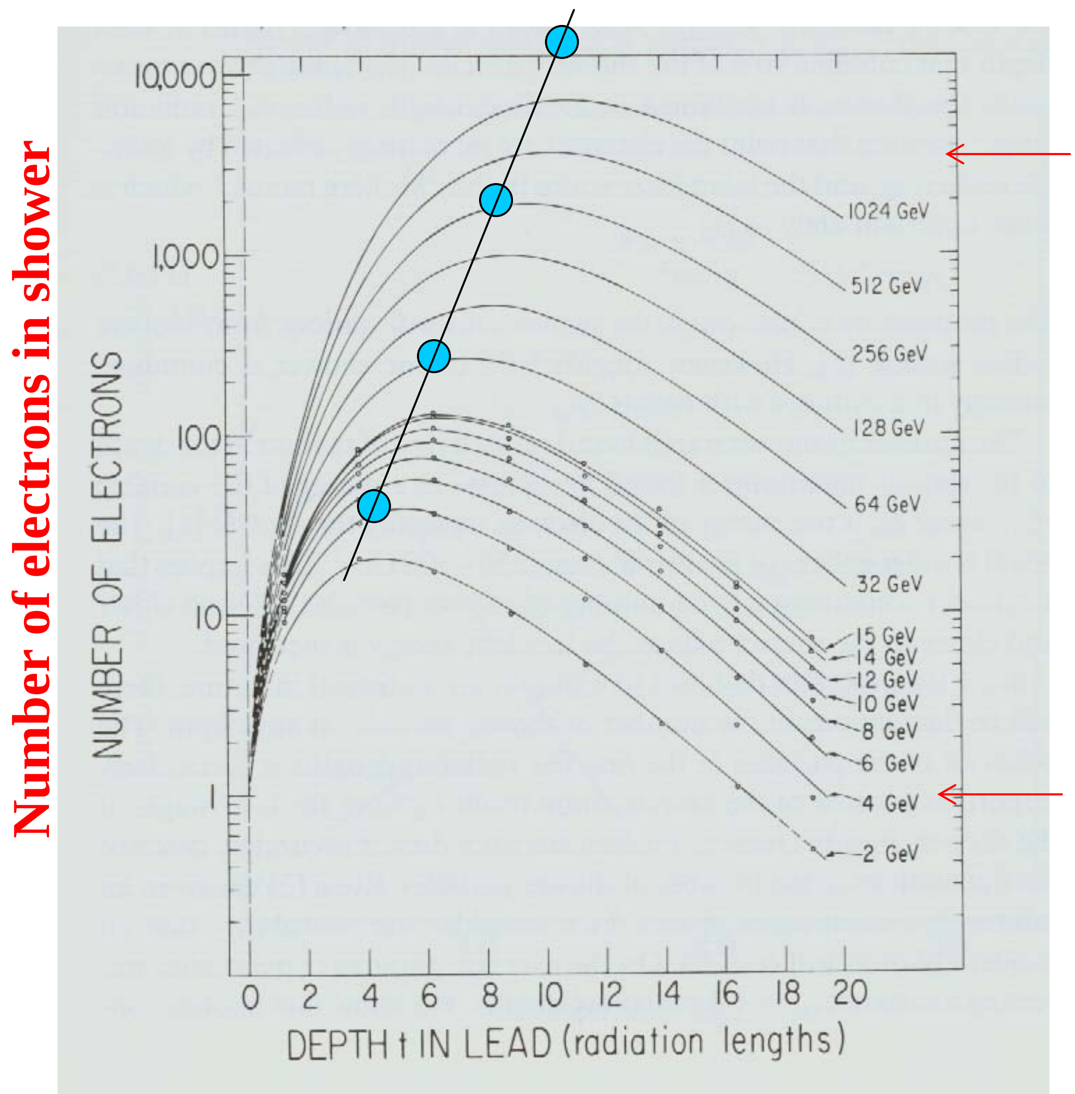

High energy electrons

Low energy electrons

- **Higher energy particles push “shower maximum” deeper into material**

- **Depth of shower maximum ∝ ln (Energy $_{e\ or\ \gamma}$)**

II.1.3 Electromagnetic cascades

Shower energy →	10 GeV		100 GeV	
Absorber ↓	$\#e^+$	E^+/E_{tot}	$\#e^+$	E^+/E_{tot}
Aluminium ($Z = 13$)	191	26%	1750	27%
Iron ($Z = 26$)	285	27%	2920	26%
Tin ($Z = 50$)	427	24%	4330	25%
Lead ($Z = 82$)	554	22%	5730	23%
Uranium ($Z = 92$)	612	23%	5970	23%

Number of positrons generated in e.m. shower development and fraction of total energy deposited by these particles.

II.1.3 Electromagnetic cascades

Composition of e.m. showers.

Shown are (%) of the energy of 10 GeV e.m. showers deposited through shower particles with energies <1 MeV (dashed), <4 MeV (dash-dotted) or >20 MeV (solid) as funtion of Z value of absorber material.

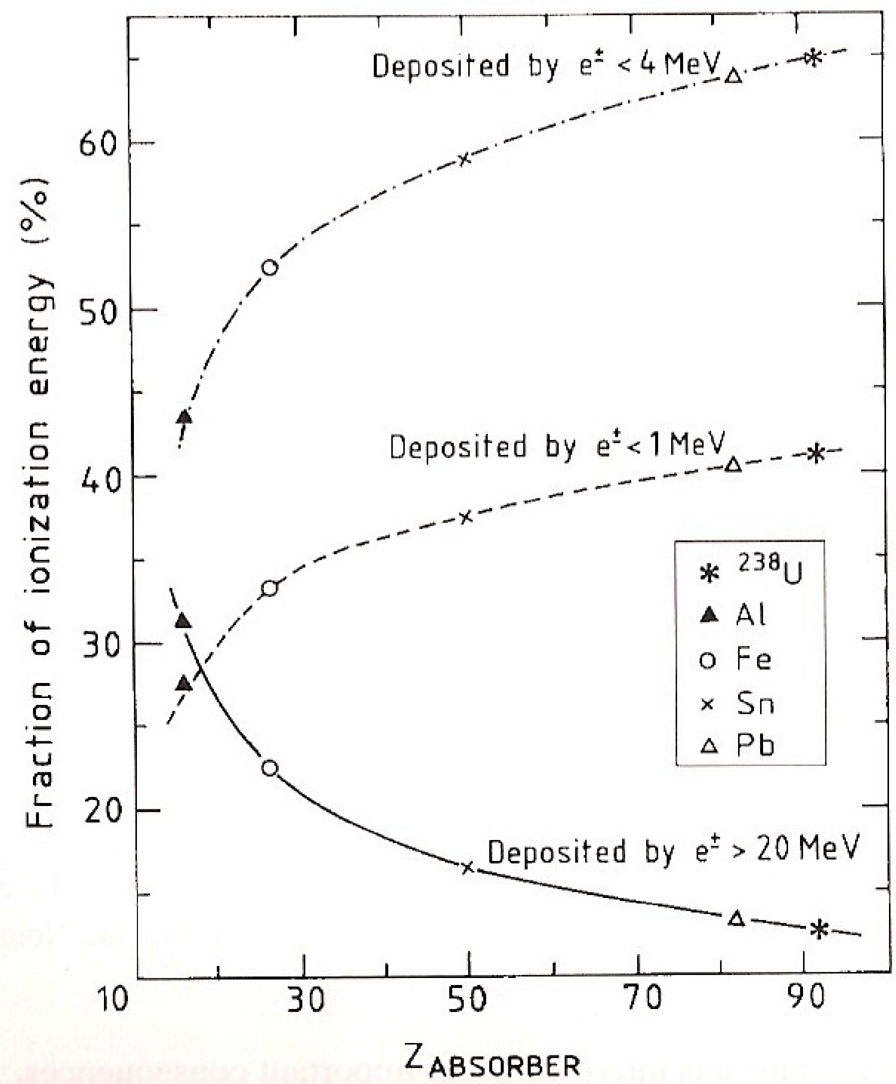

II.1.3 Electromagnetic cascades

- Transverse extension of shower

3 processes contribute to transverse dimension of electromagnetic shower

Opening angle in production process

$$\sqrt{< \Theta_\gamma^2 >} = \frac{m}{E_\gamma}$$

Multiple scattering of produced electrons

$$\sqrt{< \Theta_M^2 >} = \frac{21\ MeV}{E_e} \sqrt{\frac{x}{X_o}}$$

Main contribution due to multiple scattering of electrons with $E_e \approx \varepsilon_c$

Molière length

$$R_M = \frac{21\ MeV}{\varepsilon_c} X_o$$

characterizes transverse width of electromagnetic shower

II.1.3 Electromagnetic cascades

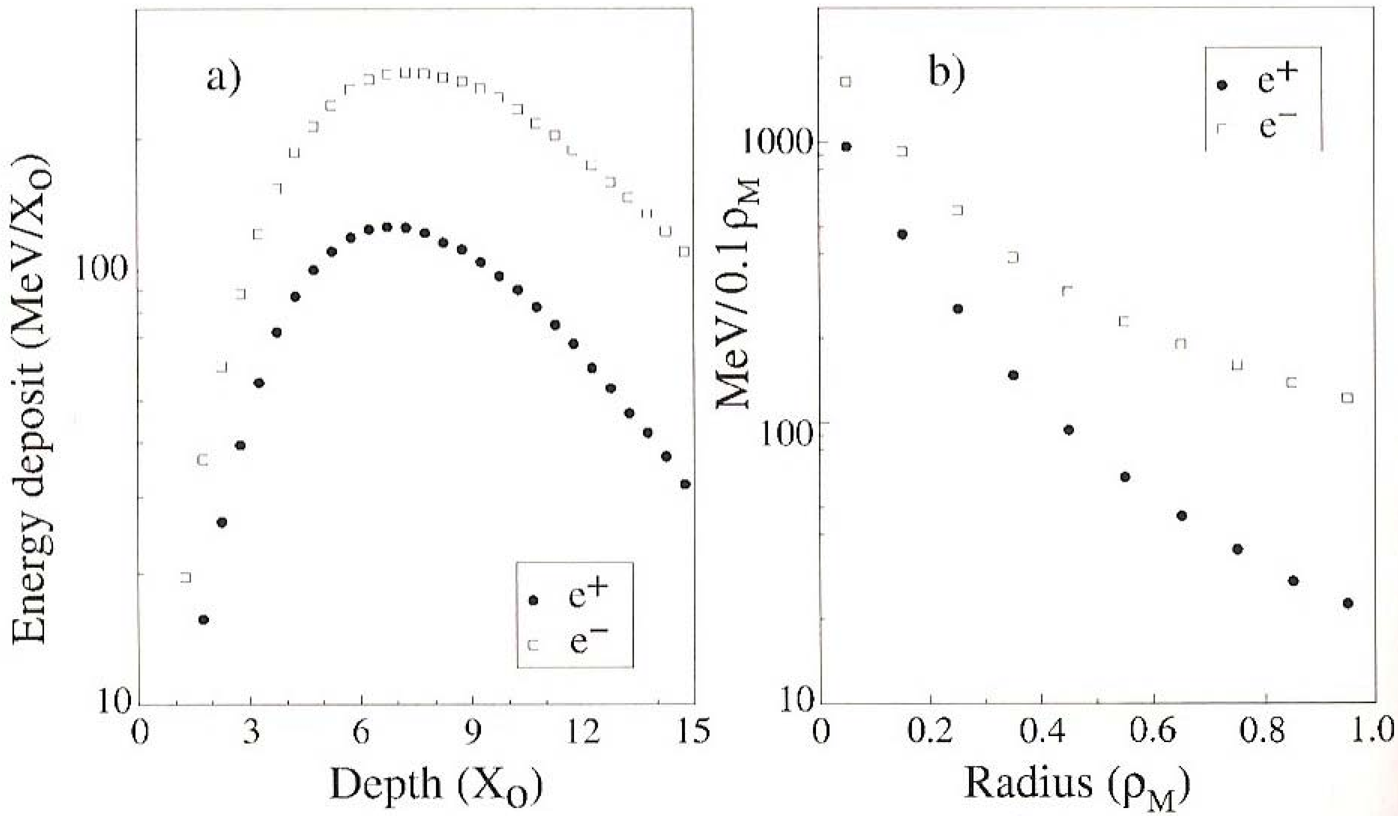

Comparison of longitudinal (a) and lateral (b) profiles of the energy deposited by electrons and positrons in 10 GeV e.m. showers in Pb.

II.1.4 Scaling variables

Useful formulas :

$$X_o = \frac{180\ A}{Z^2} \quad \frac{g}{cm^2}$$

$$\varepsilon_c = \frac{550\ MeV}{Z}$$

$$R_M = 7\ \frac{A}{Z}\ g/cm^2$$

$$t_{MAX} = ln\ \frac{E}{\varepsilon_c} - \begin{cases} 1 & e^-\ \text{induced shower} \\ 0.5 & \gamma\ \text{induced shower} \end{cases}$$

$$L\ (95\ \%)/X_o = t_{MAX} + 0.08\ Z + 9.6$$

$$R\ (95\ \%) = 2\ R_M$$

II.1.5 Electromagnetic shower profiles

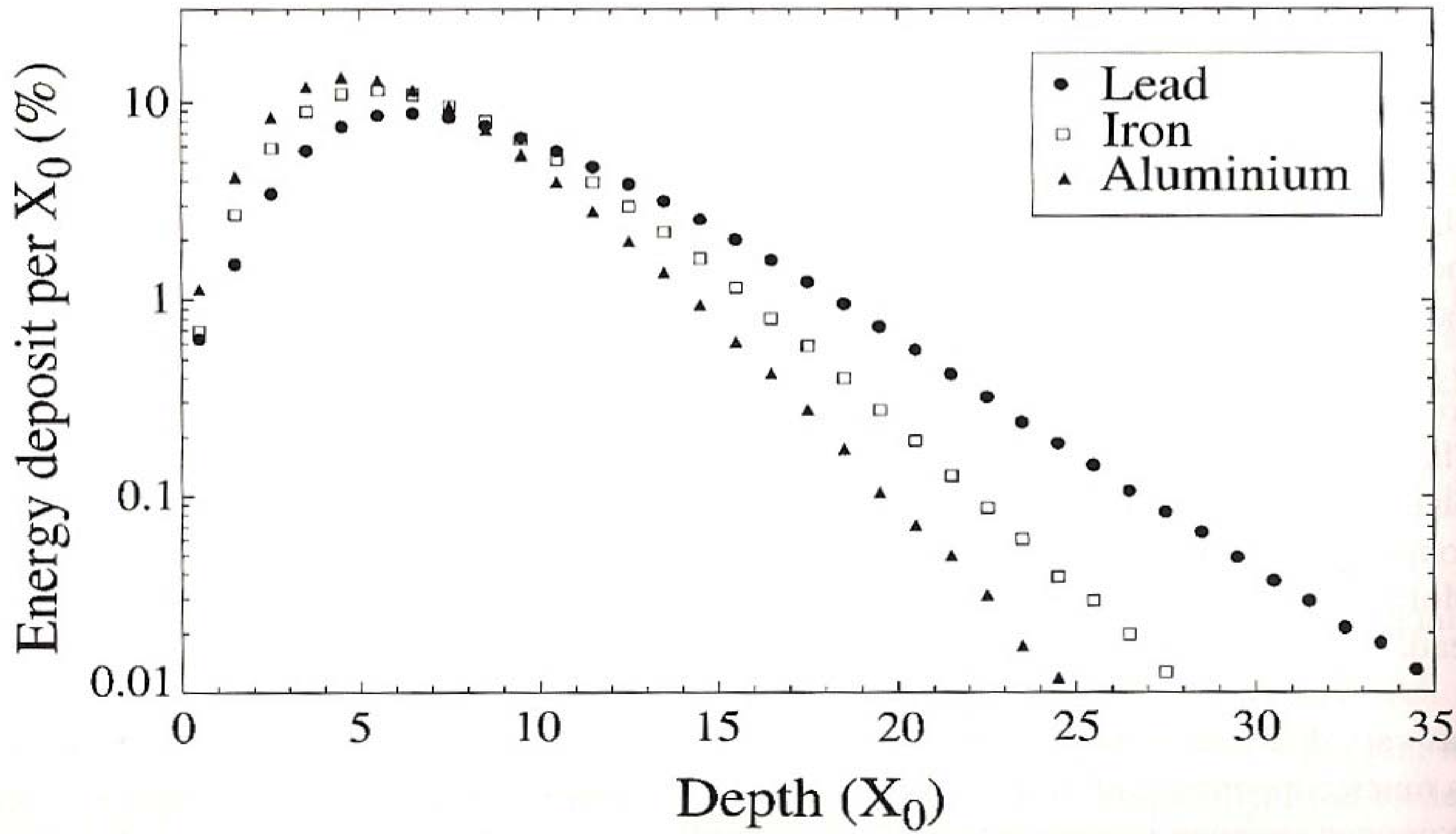

Energy deposit as a function of depth, for 10 GeV electron showers developing in Pb, Fe, Al. Show approximate scaling of longitudinal shower profile when expressed in X_0.

II.1.5 Electromagnetic shower profiles

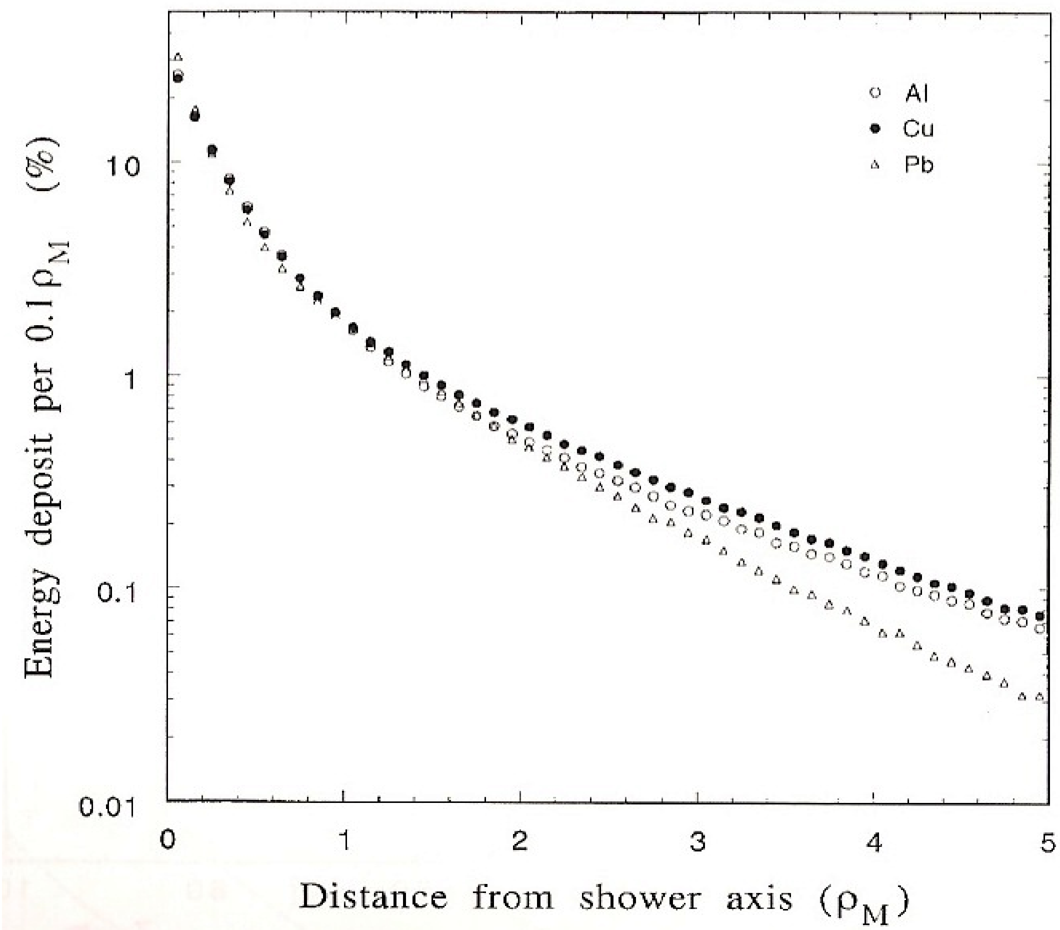

Radial energy deposit profiles for 10 GeV electrons showering in Al, Fe and Pb.

II.1.5 Electromagnetic shower profiles

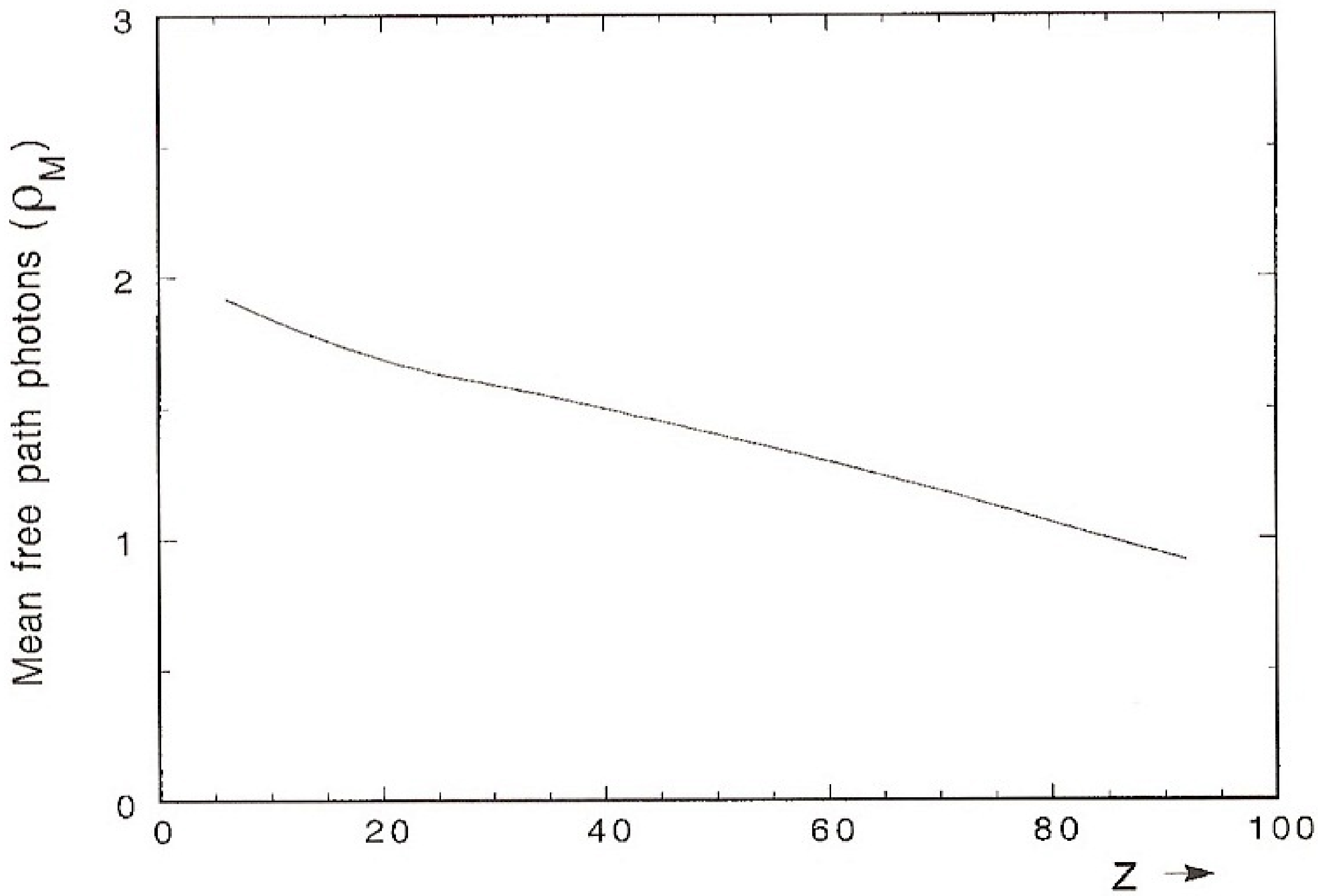

Mean free path (Molière radius ρ_M) for photons with energies 1 – 3 MeV, as function of Z.

II.1.6 Shower containment

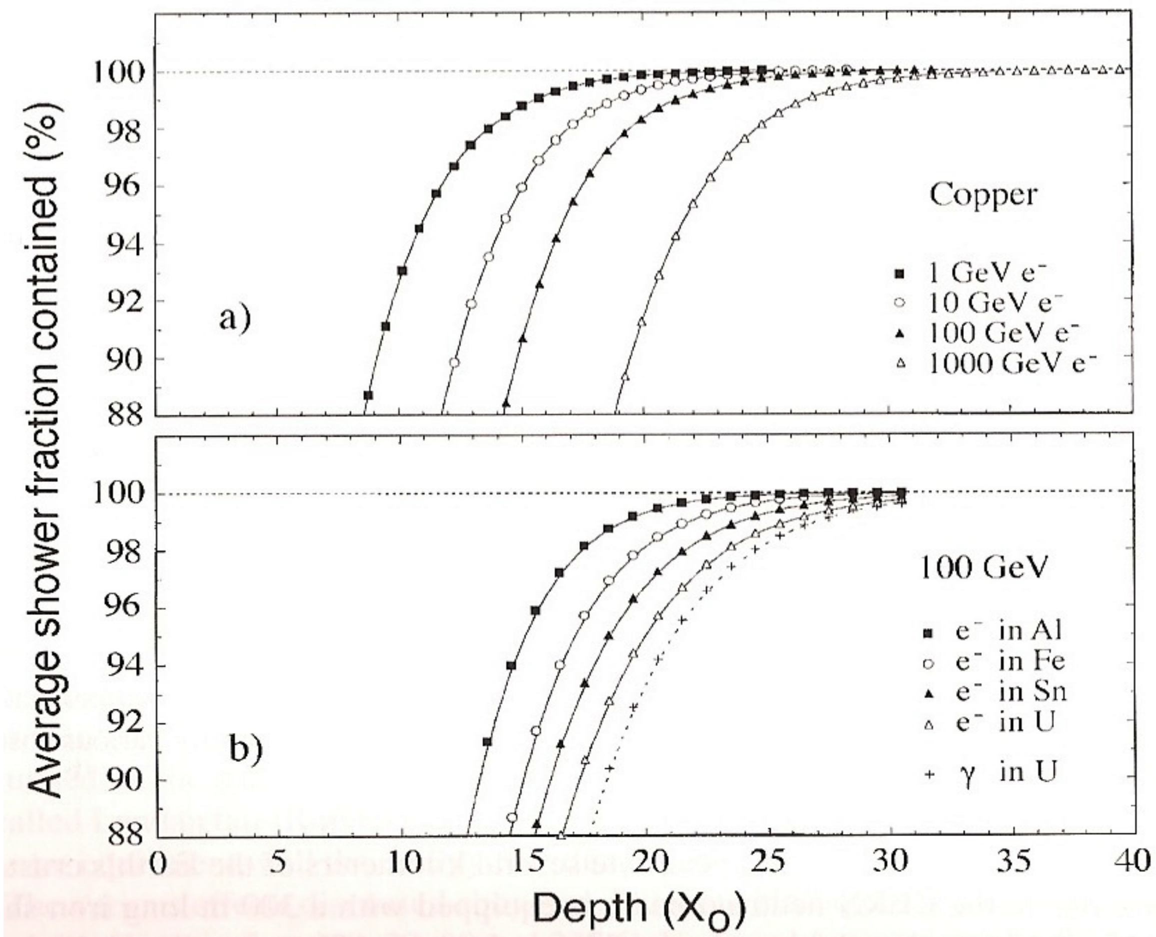

Average energy fraction contained in a block of matter with infinite transverse dimensions, as function of thickness of absorber.

(a) Results for electron showers of various energies in Cu.

(b) Results for 100 GeV electrons in different absorber materials.

II.1.6 Shower containment

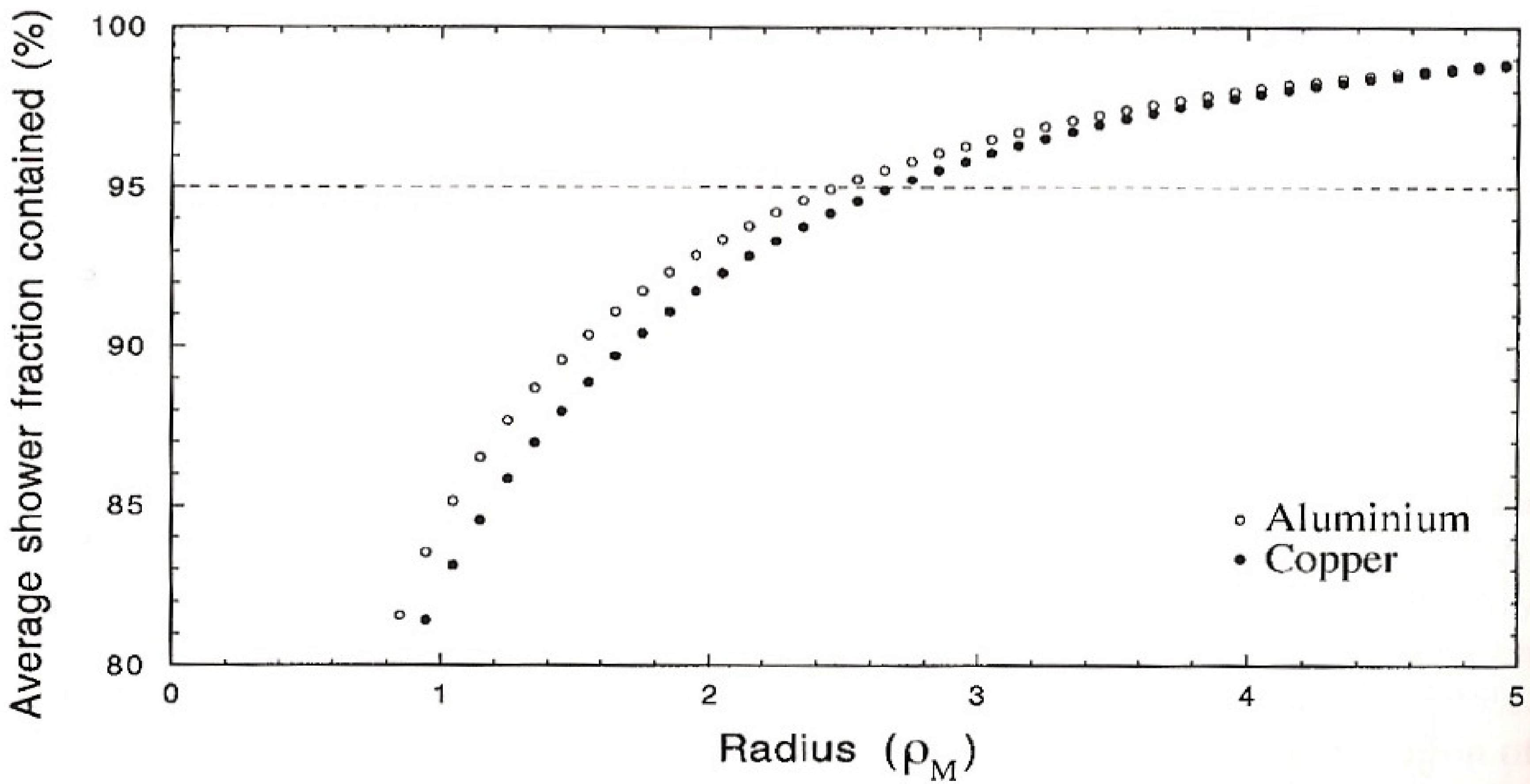

Average energy fraction contained in an infinitely long cylinder of absorber material as function of cylinder radius.

II.2 Physics of Shower Development → Muons traversing dense matter

Signal distribution for muons of different energies traversing at 3^0 incidence angle the $9.5\ \lambda_{int}$ deep SPACAL detector.

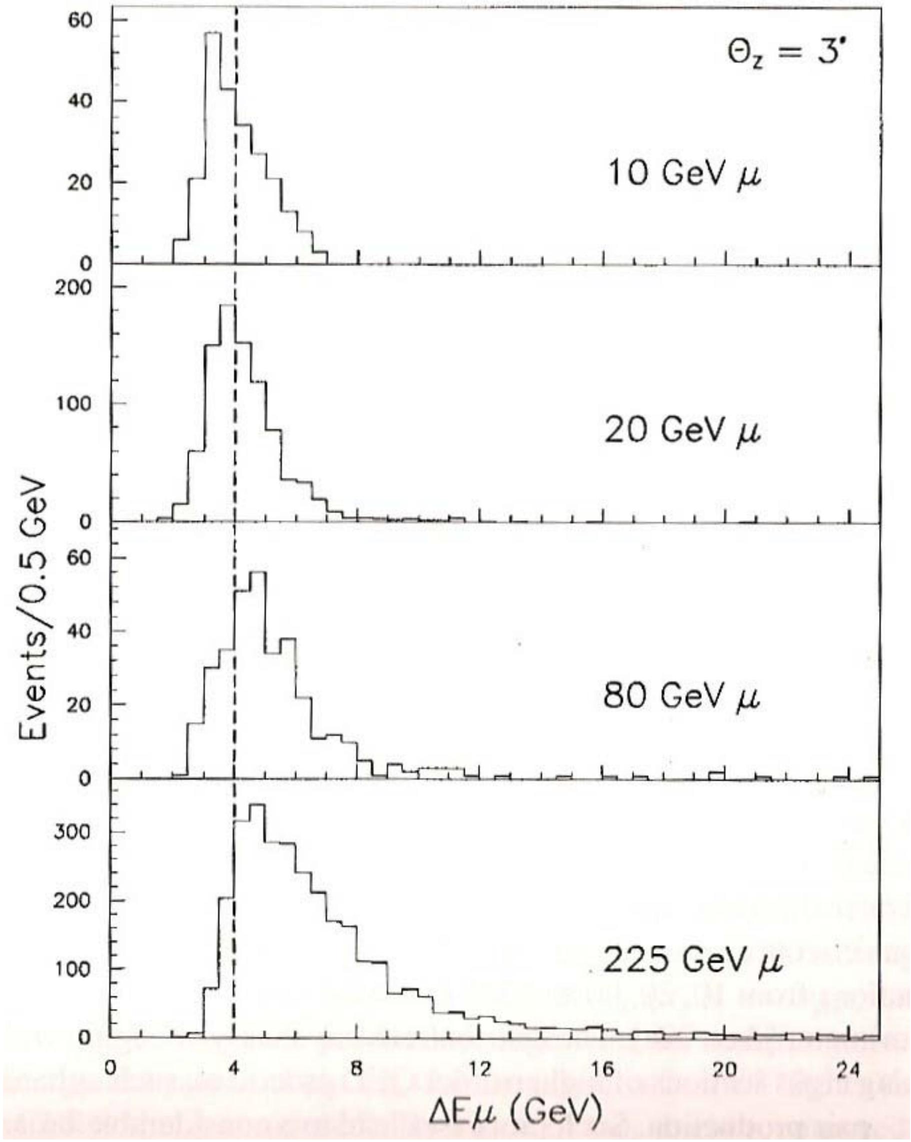

II.3 Physics of Shower Development → Hadronic showers

1. **Particle sector**
   a. E.m. decaying particles
   b. Ionization losses by charged hadrons
   c. Particle multiplicities in hadron showers
   d. Asymptotic consequences

2. **Nuclear sector**
   a. Nuclear spallation reactions
   b. Nuclear binding energy
   c. Spallation nucleons
   d. Evaporation neutrons

3. **Interactions of neutrons with matter**
   a. Elastic neutron scattering
   b. Neutron capture
   c. Production of α particles
   d. Ineleastic neutron scattering

II.3 Physics of Shower Development → Hadronic showers

4. Hadronic shower profiles

a. Nuclear interaction length

b. Longitudinal profiles

c. Lateral / radial profiles

d. Fluctuations

e. Shower profiles in Cherenkov calorimeters

5. Shower containment

II.3 Physics of Shower Development → Hadronic showers

$$p + \text{ Nucleus } \rightarrow$$

$$\underbrace{\pi^+ + \pi^- + \pi^0 + K^- + \ \dots \ + p + n +}_{\text{further reactions}} \ \dots \ + \text{ Nucleus}^*$$

Internuclear cascade + nuclear deexcitation :

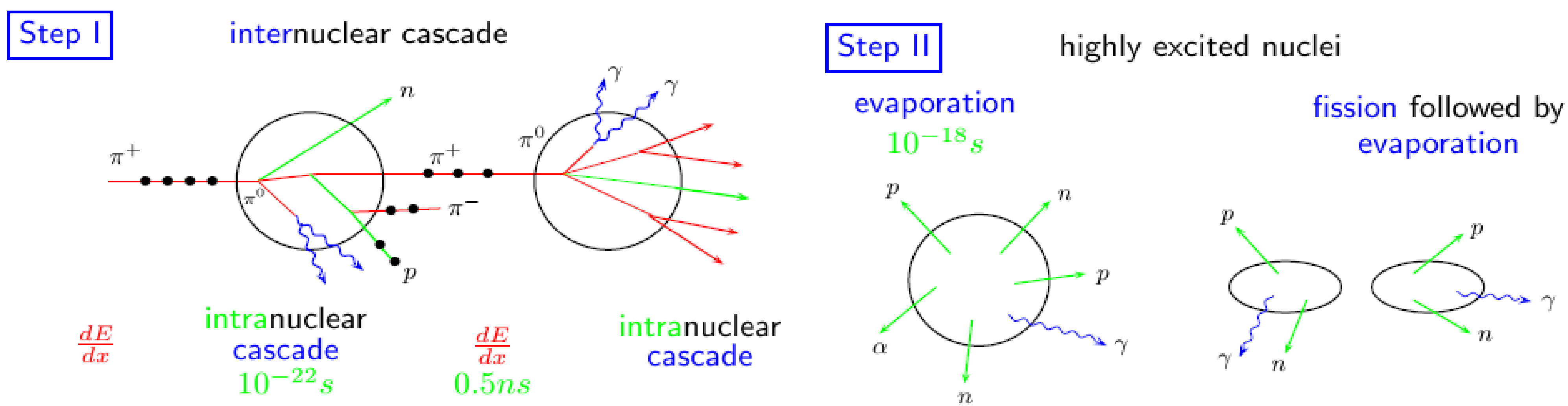

II.3.1 Particle sector → E.m. decaying particles

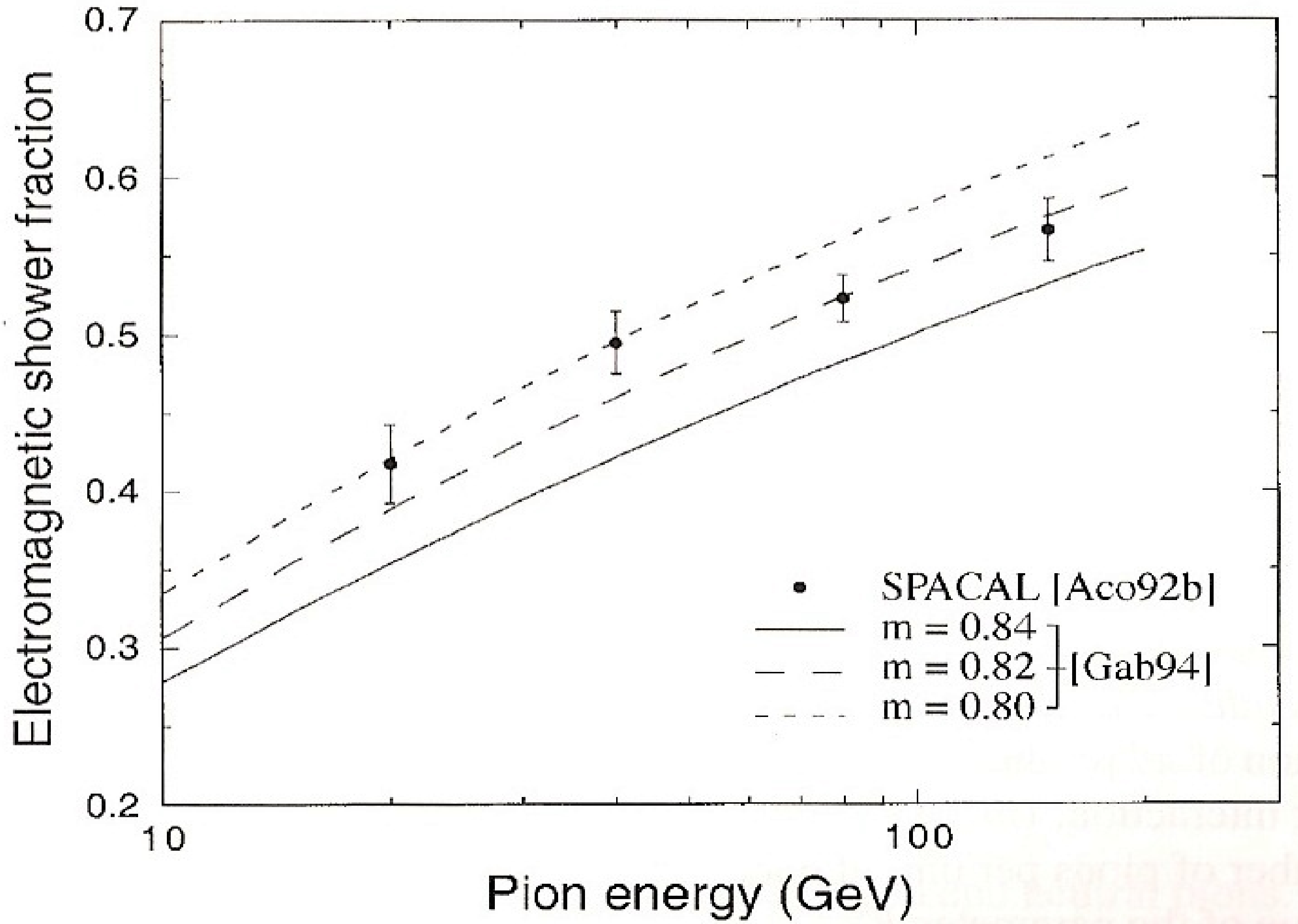

Average e.m. shower fraction, measured with SPACAL and compared to predictions.

II.3.1 Particle sector → E.m. decaying particles

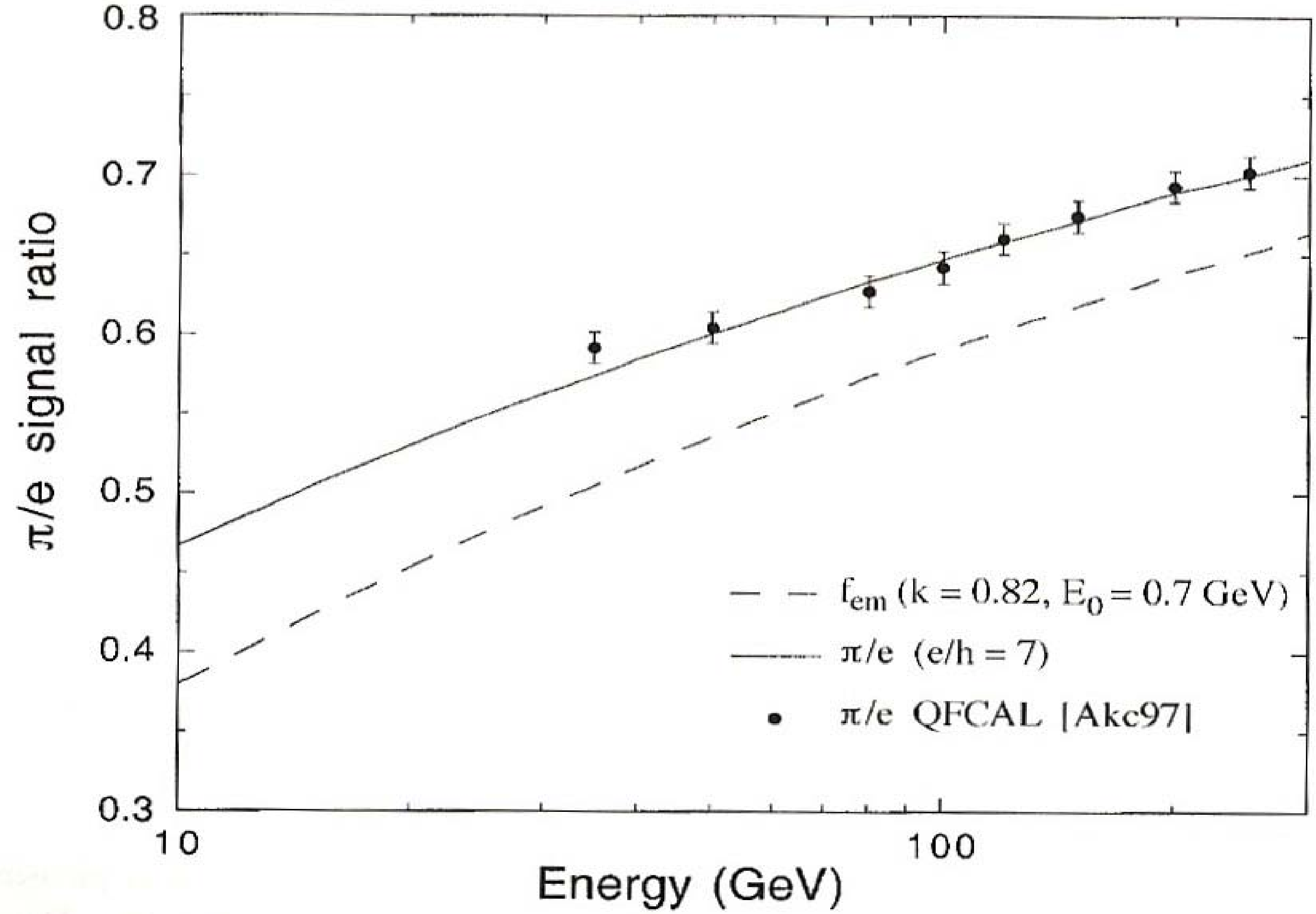

π/e signal measured with QFCAL calorimeter. Dashed curve: f_{em} fraction in the pion induced showers. Solid curve: π/e signal ratio derived from this.

II.3.1 Particle sector → E.m. decaying particles

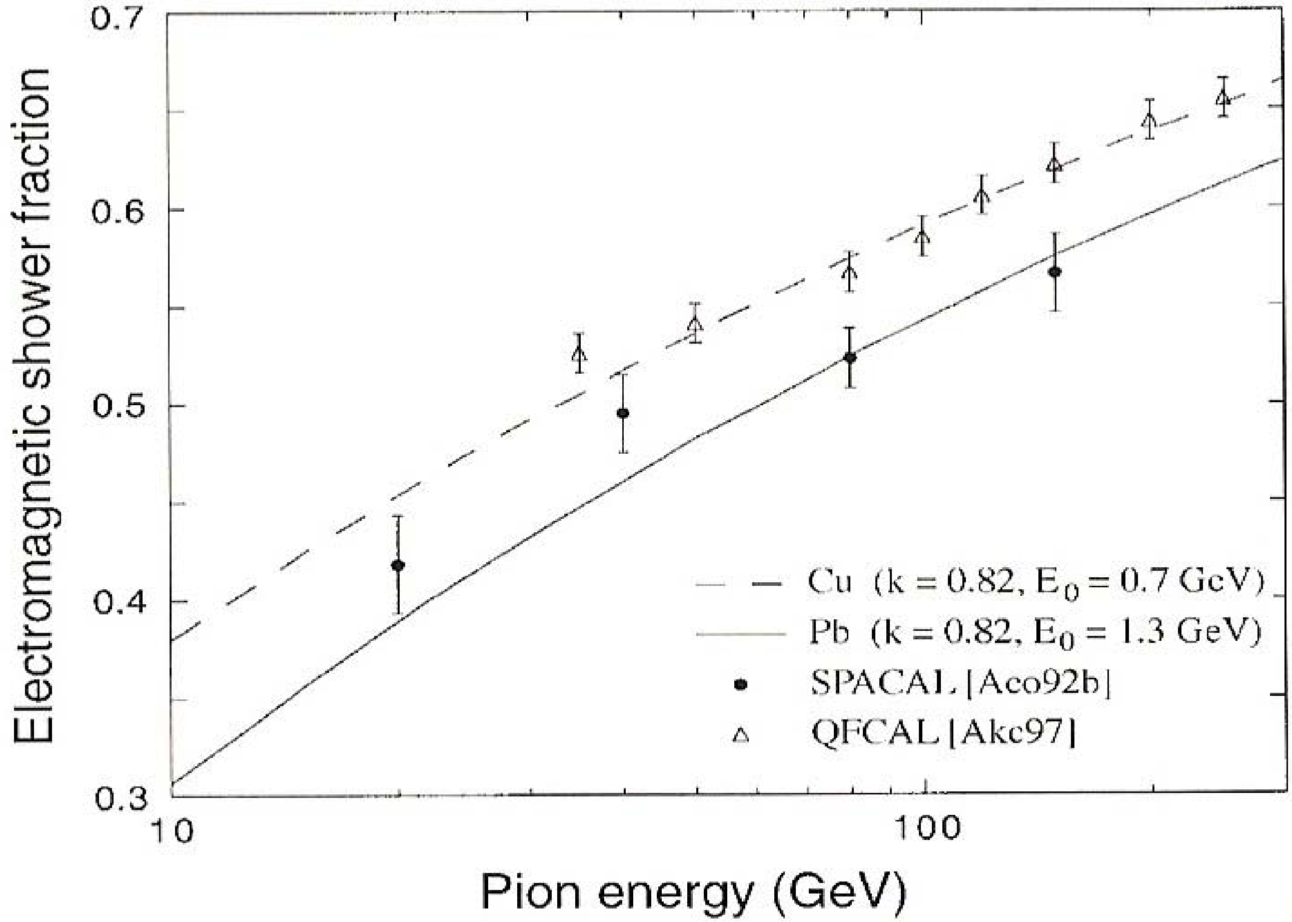

Experimental measurements of f_{em} of pion induced showers in QFCAL (Cu based) and SPACAL (Pb based).

II.3.1 Particle sector → E.m. decaying particles

QFCAL calorimeter response to p and π mesons, and ratio of these, as function of energy.

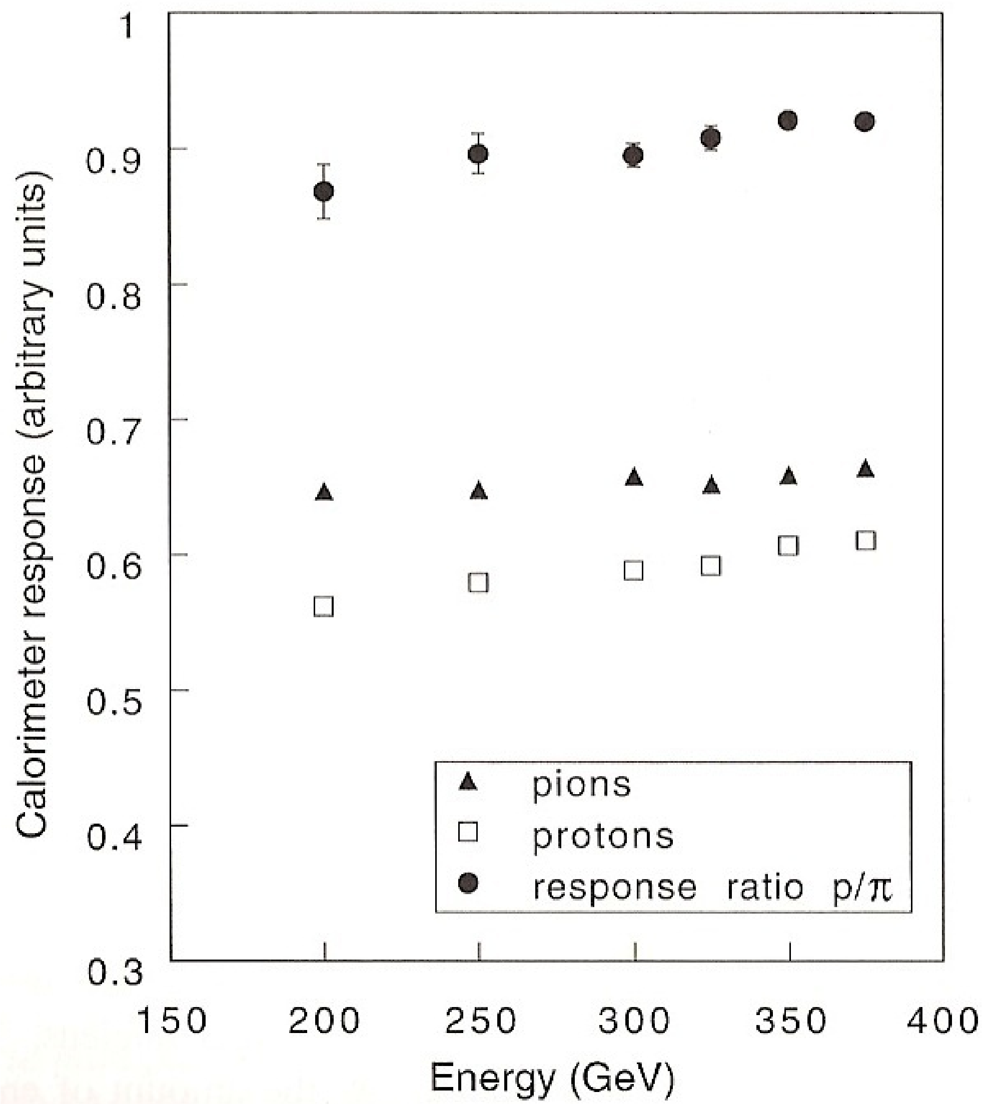

II.3.1 Particle sector → Ionization losses by charged hadrons

Absorber	Z	dE/dx (*mip*) (MeV $g^{-1}cm^2$)	λ_{int} (g cm^{-2})	$\Delta E/\lambda_{int}$ (MeV)
Carbon	6	1.745	86.3	49.5
Aluminum	13	1.615	106.4	65.9
Iron	26	1.451	131.9	90.9
Copper	29	1.403	134.9	96.2
Tin	50	1.264	163	129
Tungsten	74	1.145	185	162
Lead	82	1.123	194	173
Uranium	92	1.082	199	184

Ionization energy loss of minimum ionizing hadrons in various absorber materials.

II.3.1 Particle sector → Multiplicities in hadron showers

E_π (GeV)	$\langle f_{\rm em} \rangle$	$\langle \#\pi^{\pm}, K... \rangle$	$\langle \#\pi^0 \rangle$
10	0.380 (0.307)	9 (5)	3 (2)
20	0.453 (0.389)	16 (9)	5 (3)
30	0.492 (0.432)	22 (13)	7 (4)
50	0.536 (0.482)	33 (20)	11 (7)
80	0.574 (0.524)	49 (29)	16 (10)
100	0.591 (0.542)	58 (35)	19 (12)
150	0.619 (0.575)	82 (49)	27 (16)
200	0.639 (0.596)	103 (62)	34 (21)
300	0.664 (0.624)	144 (87)	48 (29)
400	0.681 (0.643)	182 (110)	61 (37)
500	0.694 (0.657)	219 (132)	73 (44)
700	0.712 (0.678)	288 (173)	96 (58)
1000	0.730 (0.698)	386 (232)	129 (77)

Characteristics of particle production in pion induced showers in Cu (Pb).

II.3.1 Particle sector → Asymptotic consequences

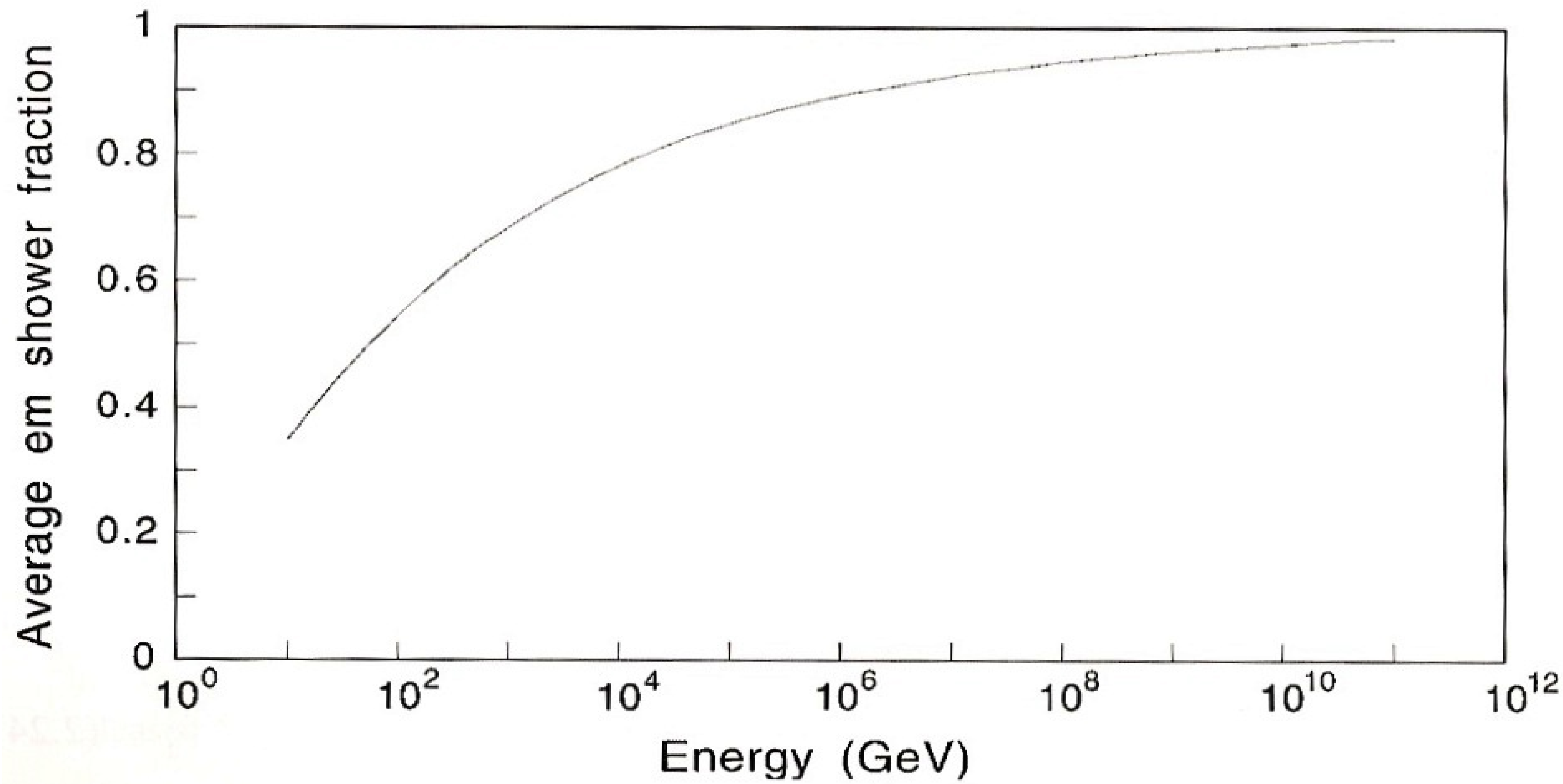

Average fraction of the initial energy carried by the e.m. shower component, as function of the initial energy.

II.3.2 Nuclear sector → Nuclear spallation reactions

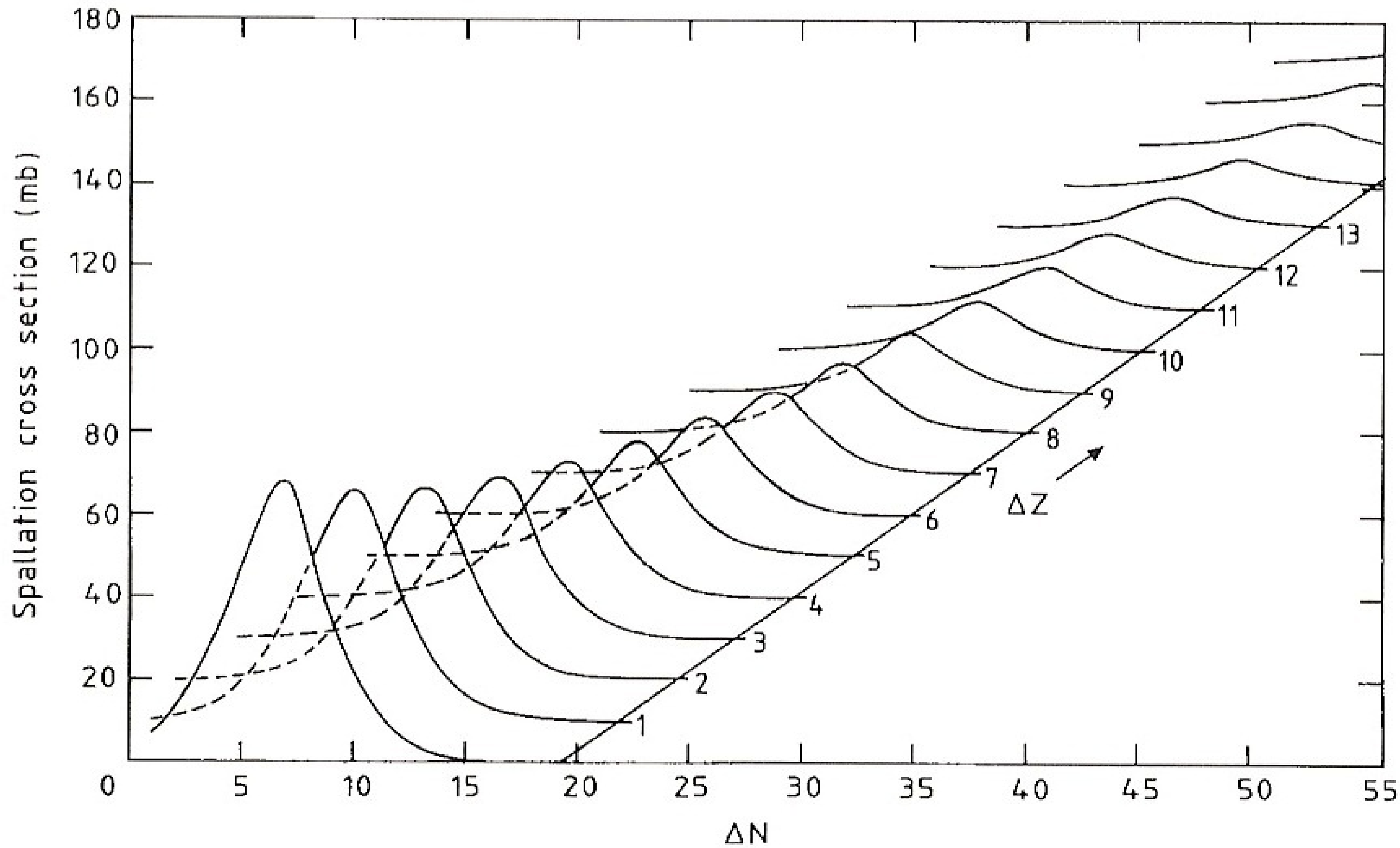

Cross section for nuclides produced by spallation of ^{238}U induced by 2 GeV hadron. The final state nuclide is defined by the number of protons (ΔZ) and neutrons (ΔN) released from the target nucleus.

II.3.2 Nuclear sector → Nuclear binding energy

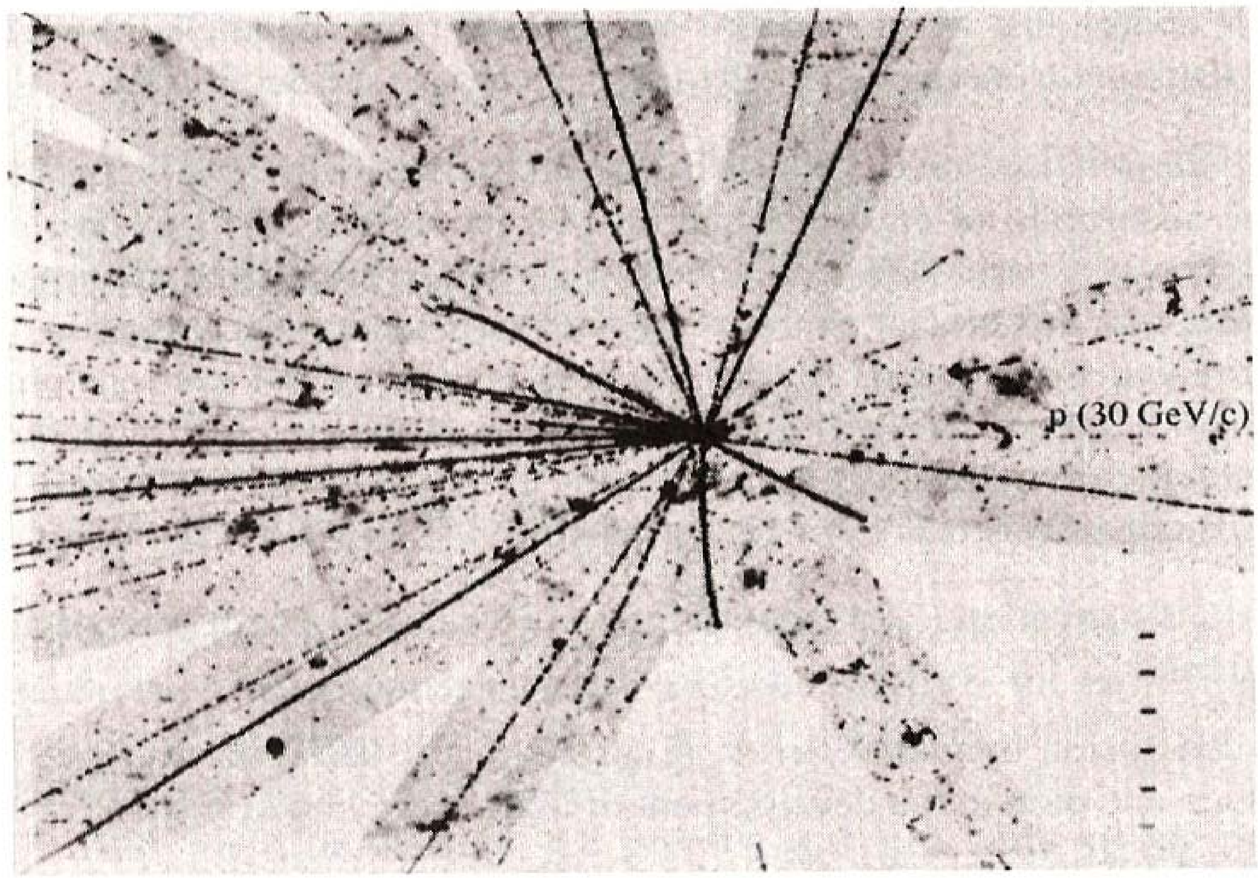

A proton-nucleus interaction in a nuclear emulsion stack.

II.3.2 Nuclear sector → Spallation nucleons

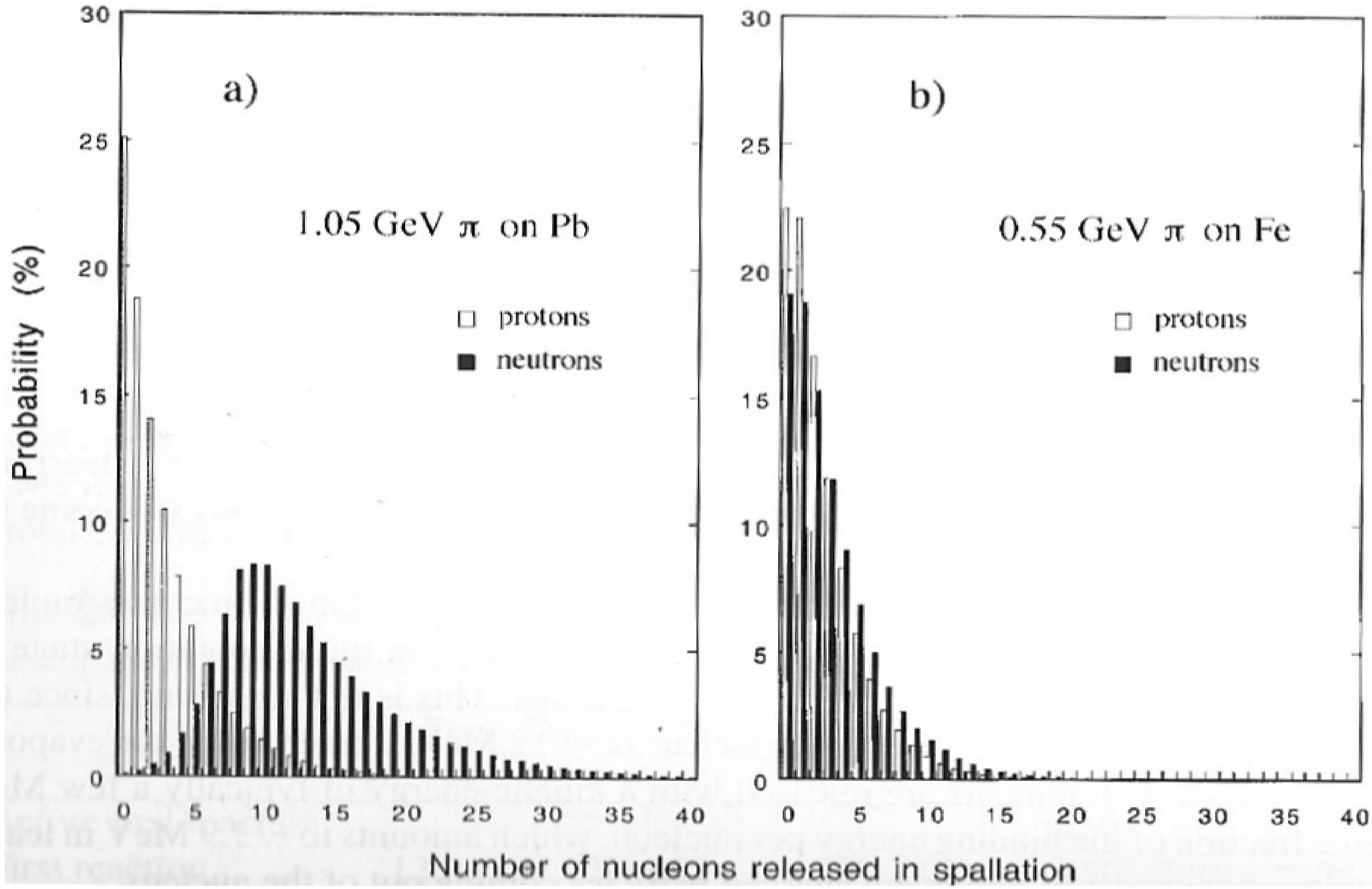

Distribution of the number of protons and neutrons produced in spallation reactions induced by 1.05 GeV pions on Pb and by 0.55 GeV pions on Fe.

II.3.2 Nuclear sector → Spallation nucleons

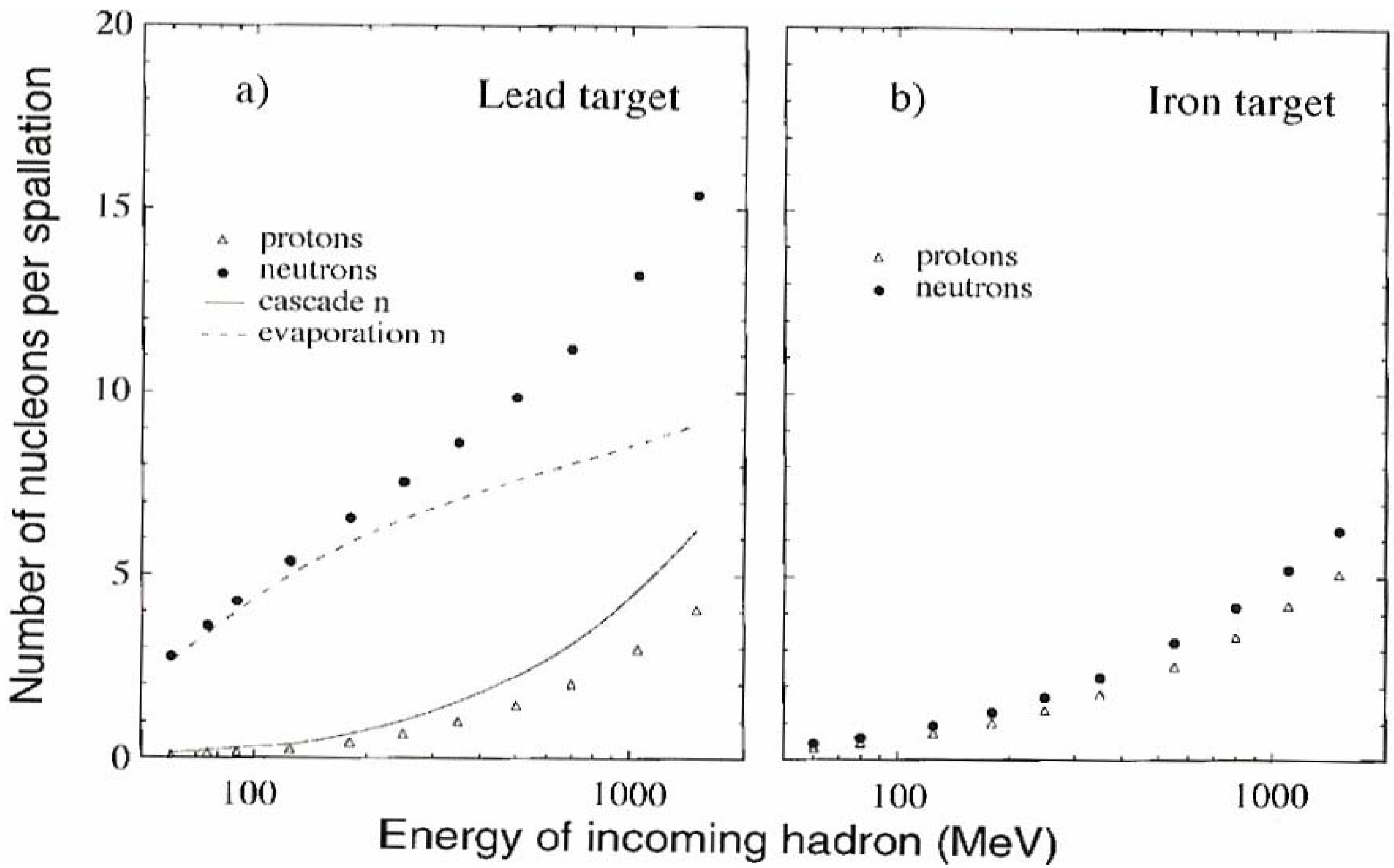

E number of protons and neutrons produced in spallation reactions on Pb and Fe as function of the energy of incoming hadrons.

II.3.2 Nuclear sector → Spallation nucleons

	Binding energy	*Evaporation n* (# neutrons)	*Cascade n* (# neutrons)	*Ionization* (# cascade p)	*Target recoil*
Before first reaction				(250) (π_{in})	
First reaction	126	27 (9)	519 (4.2)	350 (2.8)	28
Generation 2	187	63 (21)	161 (1.7)	105 (1.1)	3
Generation 3	77	24 (8)	36 (1.1)	23 (0.7)	1
Generation 4	24	12 (3)			
Total	414	126 (41)		478 (4.6)	32

Destination of the 1.3 GeV total energy carried by an average pion produced in hadronic shower development in Pb.

II.3.2 Nuclear sector → Spallation nucleons

Energy deposit and composition of the non e.m. component of hadronic showers in Pb and Fe.

	Lead	*Iron*
Ionization by pions	19%	21%
Ionization by protons	37%	53%
Total ionization	56%	74%
Nuclear binding energy loss	32%	16%
Target recoil	2%	5%
Total invisible energy	34%	21%
Kinetic energy evaporation neutrons	10%	5%
Number of charged pions	0.77	1.4
Number of protons	3.5	8
Number of cascade neutrons	5.4	5
Number of evaporation neutrons	31.5	5
Total number of neutrons	36.9	10
Neutrons/protons	10.5/1	1.3/1

II.3.2 Nuclear sector → Spallation nucleons

Deposition of non-em energy	*Lead* Table 2.5	*Lead* [Gab85]	*Iron* Table 2.5	*Iron* [Gab85]
Ionization by pions	19%	13.3%	21%	14.4%
Ionization by protons	37%	33.4%	53%	42.5%
Kinetic energy evaporation neutrons	10%	12.2%	5%	7.8%
Excitation γs		2.5%		3.4%
Total invisible energy	34%	38.6%	21%	31.8%

Where does the energy carried by the non-e.m. component of hadronic showers go?

II.3.2 Nuclear sector → Evaporation neutrons

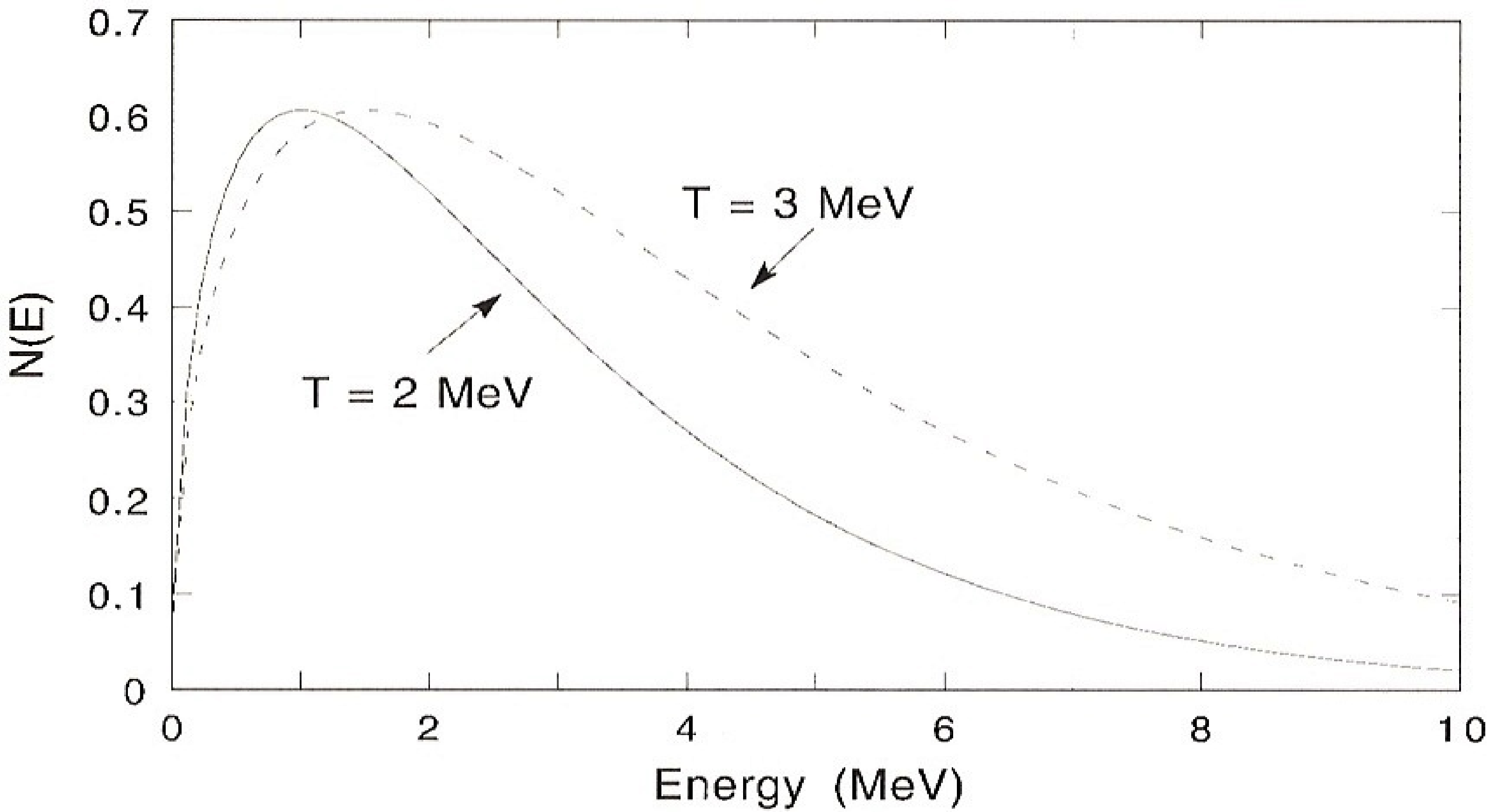

Kinetic energy spectrum of evaporation neutrons, produced according to Maxwell distributions with temperatures of 2 MeV and 3 MeV respectively.

II.3.2 Nuclear sector → Evaporation neutrons

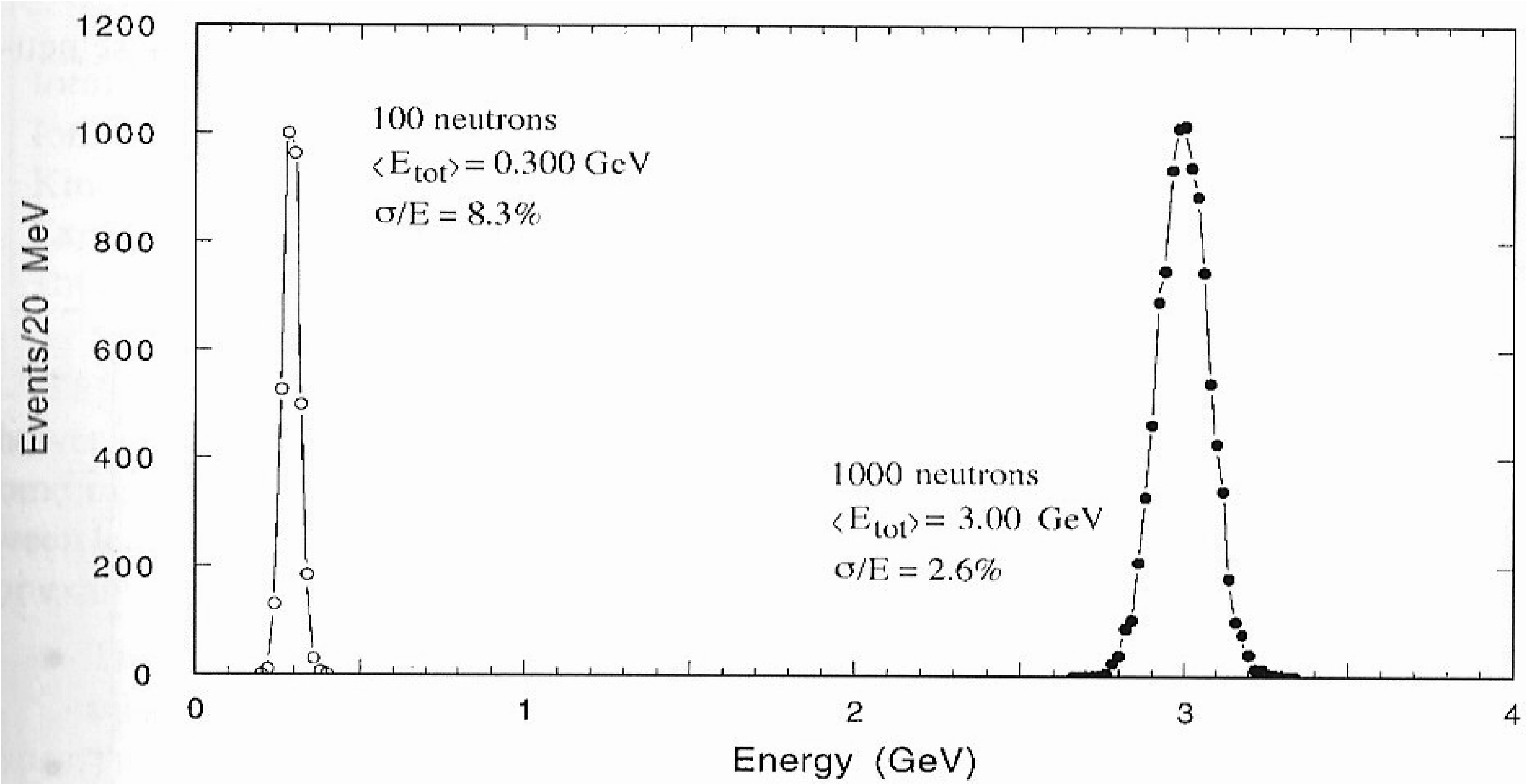

Distribution of the total kinetic energy carried by 100 and 1000 evaporation neutrons.

II.3.3 n interactions with matter

a. **Elastic n scattering**

b. **n capture**

c. **Production of α particles**

d. **Inelastic n scattering**

II.3.4 Hadronic shower profiles → Nuclear interaction length

typical length scale : interaction length

$$\lambda_{int} = \frac{1}{\frac{L\cdot\rho}{A}\cdot\sigma_{int}} = \frac{A}{\sigma_{pN}A^{2/3}\cdot L\cdot\rho} \sim A^{1/3}$$

II.3.4 Hadronic shower profiles → An Experiment

No simple model but elegant experiment :

C. Leroy, Y. Sirois, R. Wigmans   NIM A 252 (1986) 4

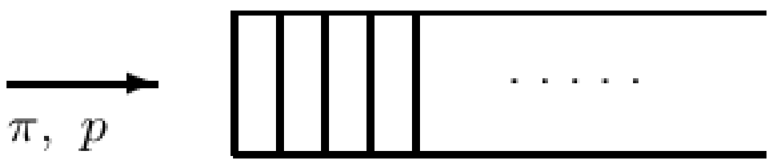

IDEA :
- Stack of ^{238}U–plates (3 mm thick)
- Induced radioactivity fingerprint of reactions frozen into block
- E_γ and $T_{1/2}$ helps to identify produced nuclei
- ^{239}Np slow n–capture in ^{238}U
  ^{237}U nuclear reaction $(n, 2n)$, (γ, n), (p, α) ...
  $^{140}Ba,\ ^{131}I,\ ^{90}Mo, \ldots$ nuclear fission

II.3.4 Hadronic shower profiles → Longitudinal profiles

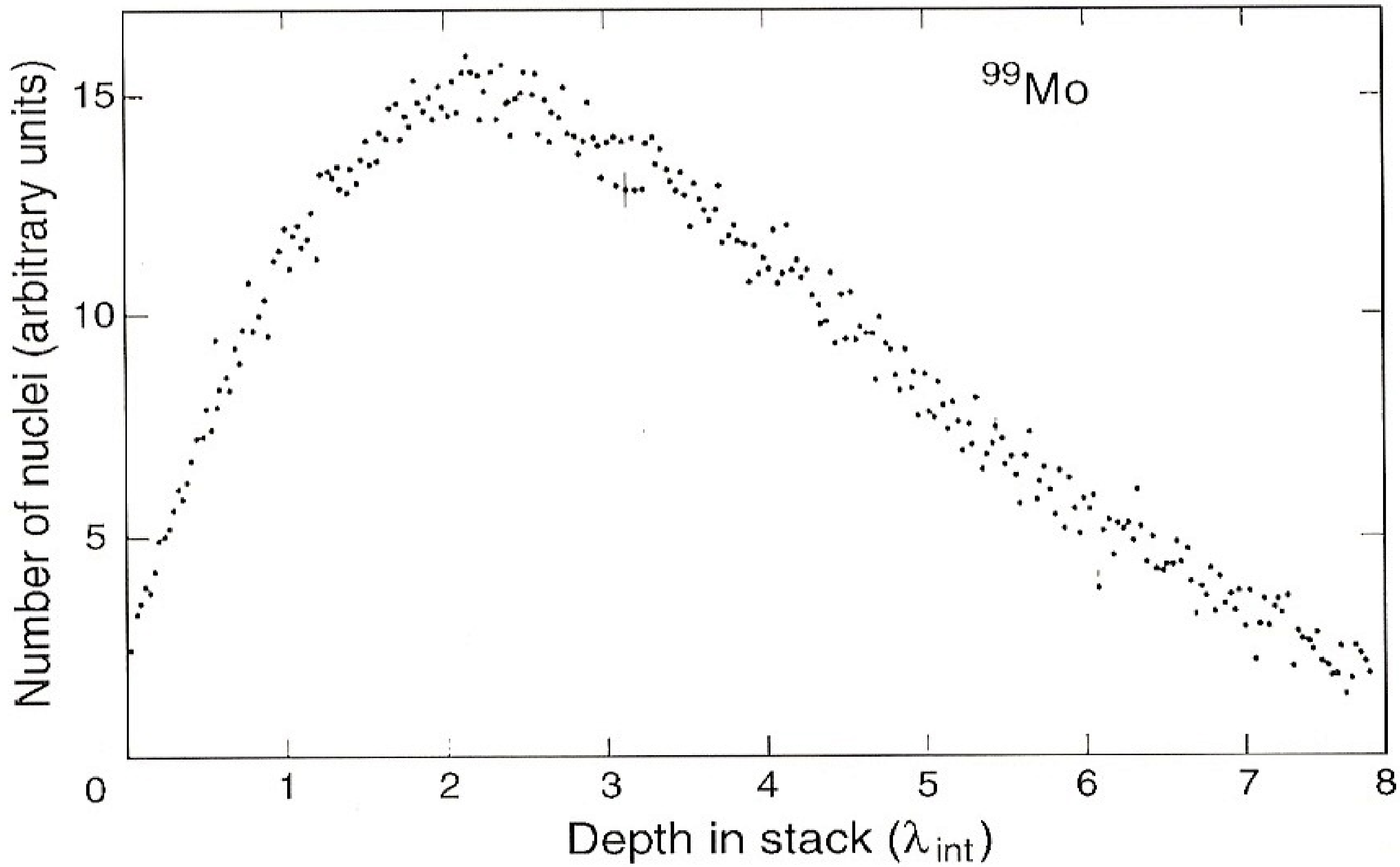

Longitudinal shower profile for 300 GeV π^- interactions in a block of U, measured from the induced radioactivity.

II.3.4 Hadronic shower profiles → Lateral / radial profiles

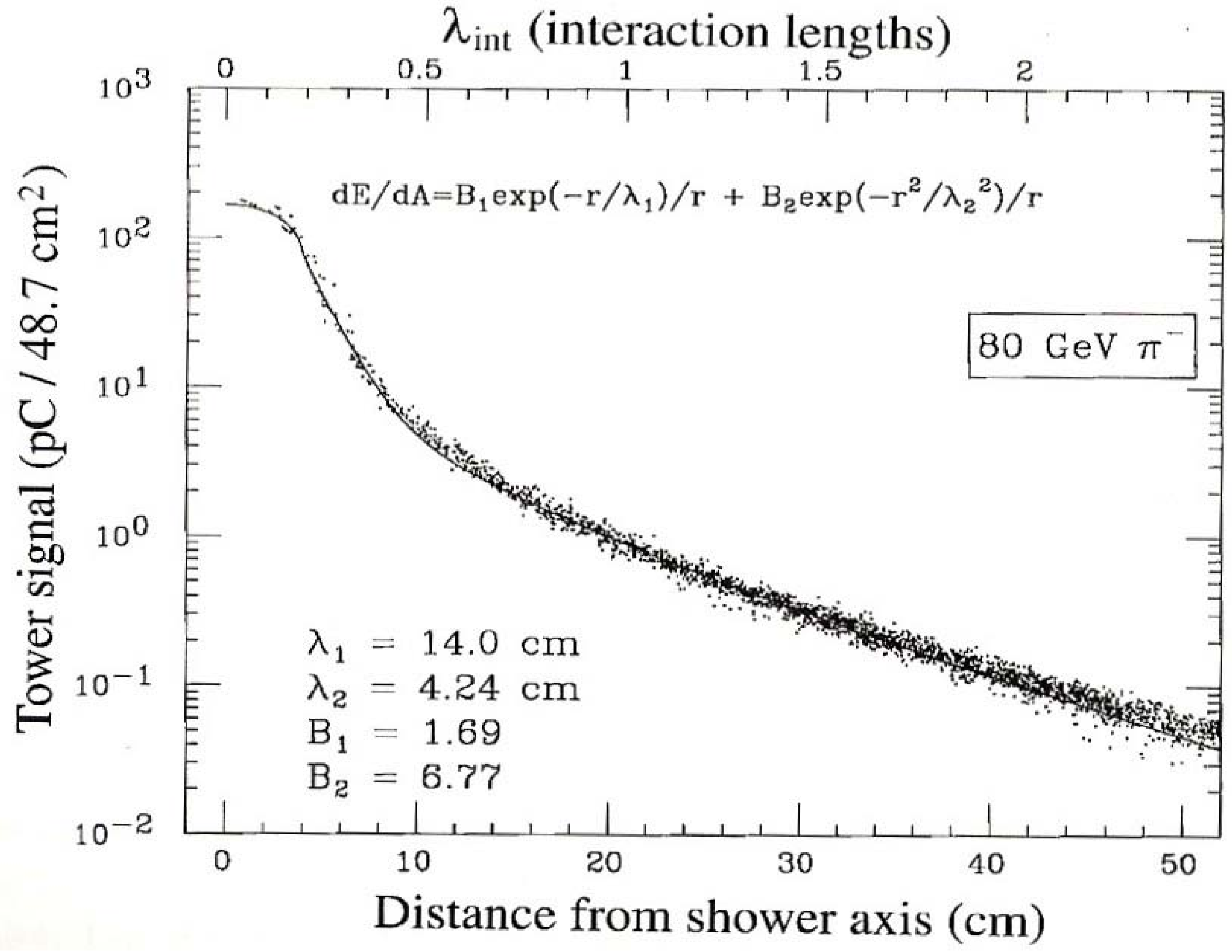

Average lateral profile of the energy deposited by 80 GeV π^- showering in the SPACAL detector.

II.3.4 Hadronic shower profiles → Lateral / radial profiles

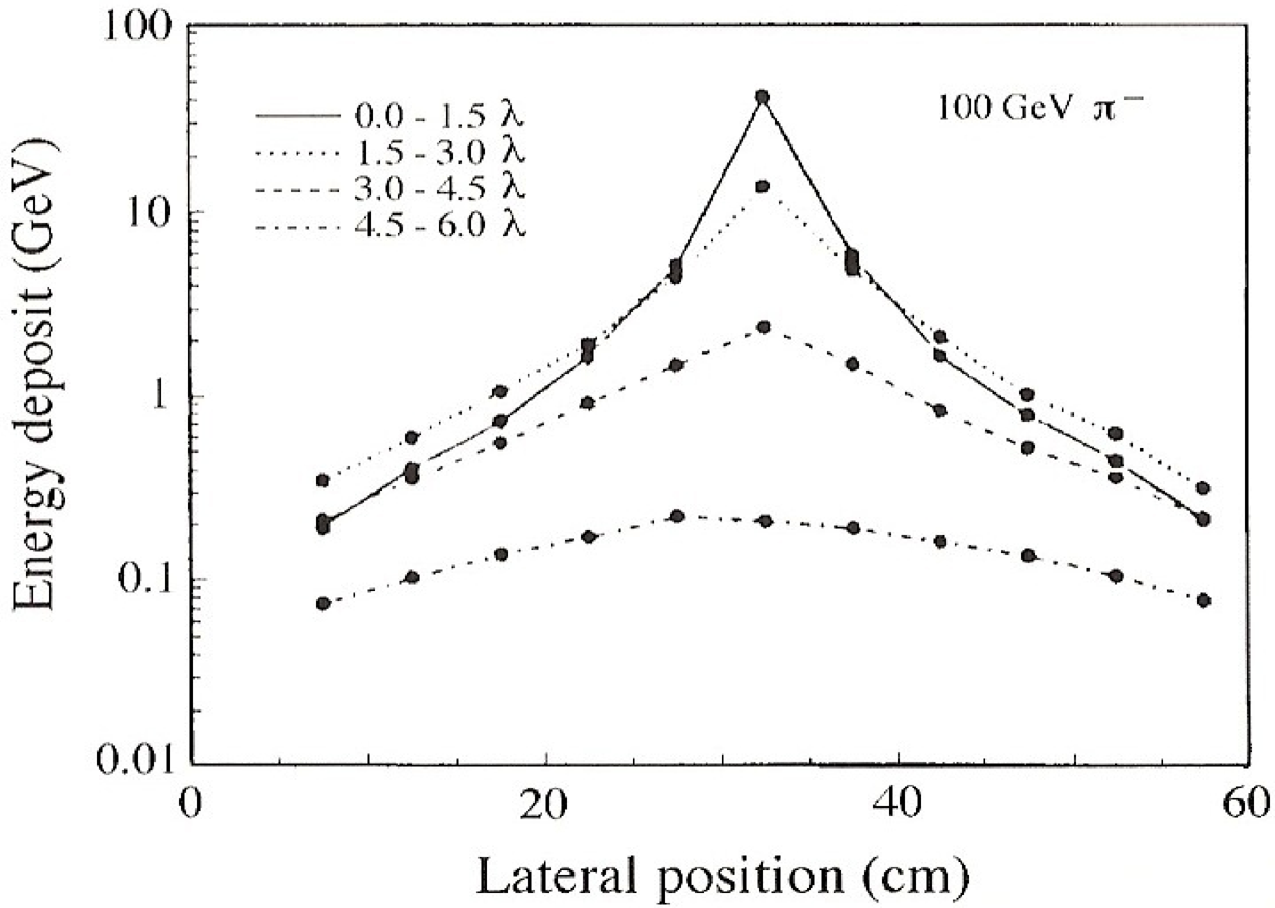

Lateral profiles for pion induced showers, measured at different depths, with the ZEUS calorimeter.

II.3.4 Hadronic shower profiles → Lateral / radial profiles

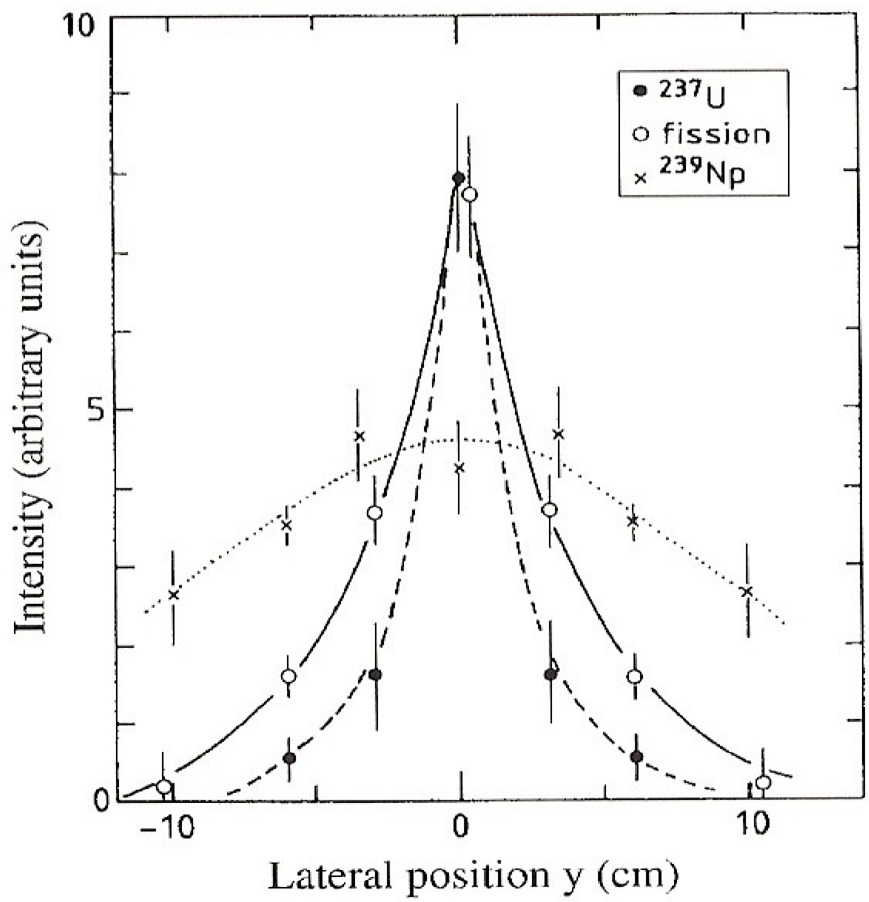

Lateral profiles for 300 GeV π^- interactions in a block of U, measured from the induced radioactivity at a depth of 4 λ_{int} inside the block.

II.3.4 Hadronic shower profiles → Profiles in Cherenkov cal.

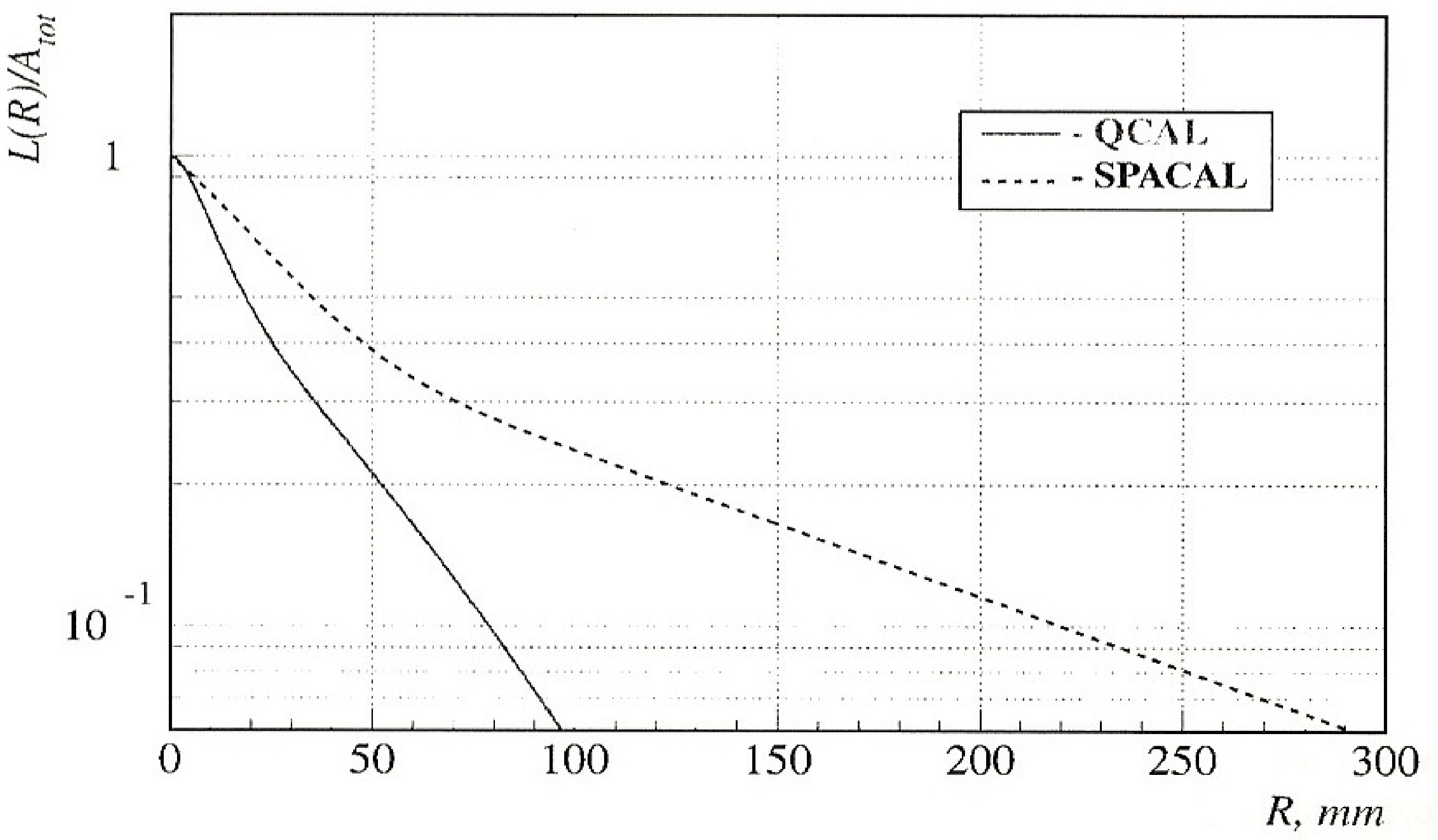

Comparison of transverse characteristics of 80 GeV π^- showers measured with a scintillation calorimeter and with a Cherenkov calorimeter.

II.3.5 Shower containment

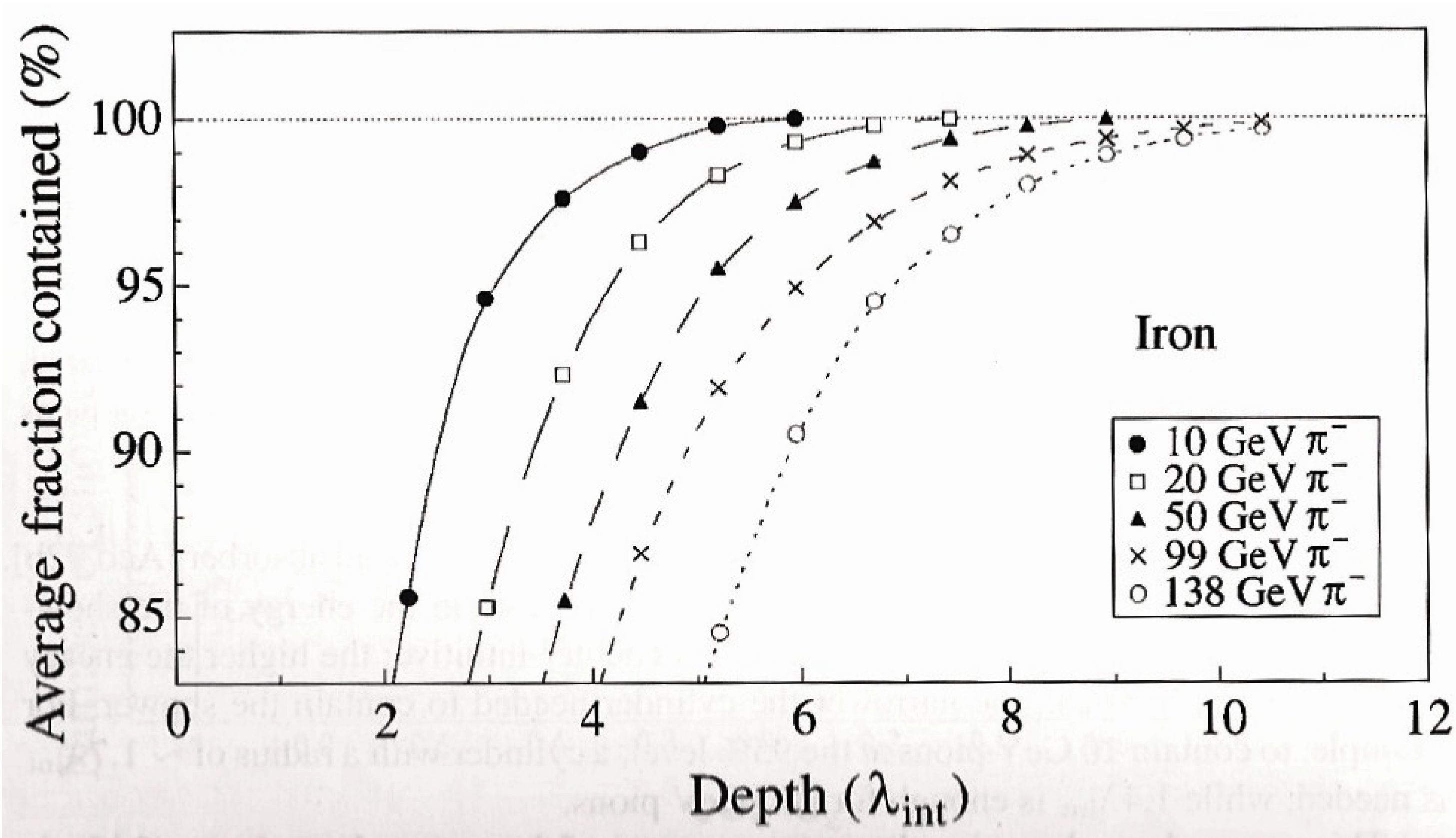

Average energy fraction contained in ablock of matter with infinite transverse dimensions, as function of the thickness of this absorber, expressed in λ_{int} .

II.3.5 Shower containment

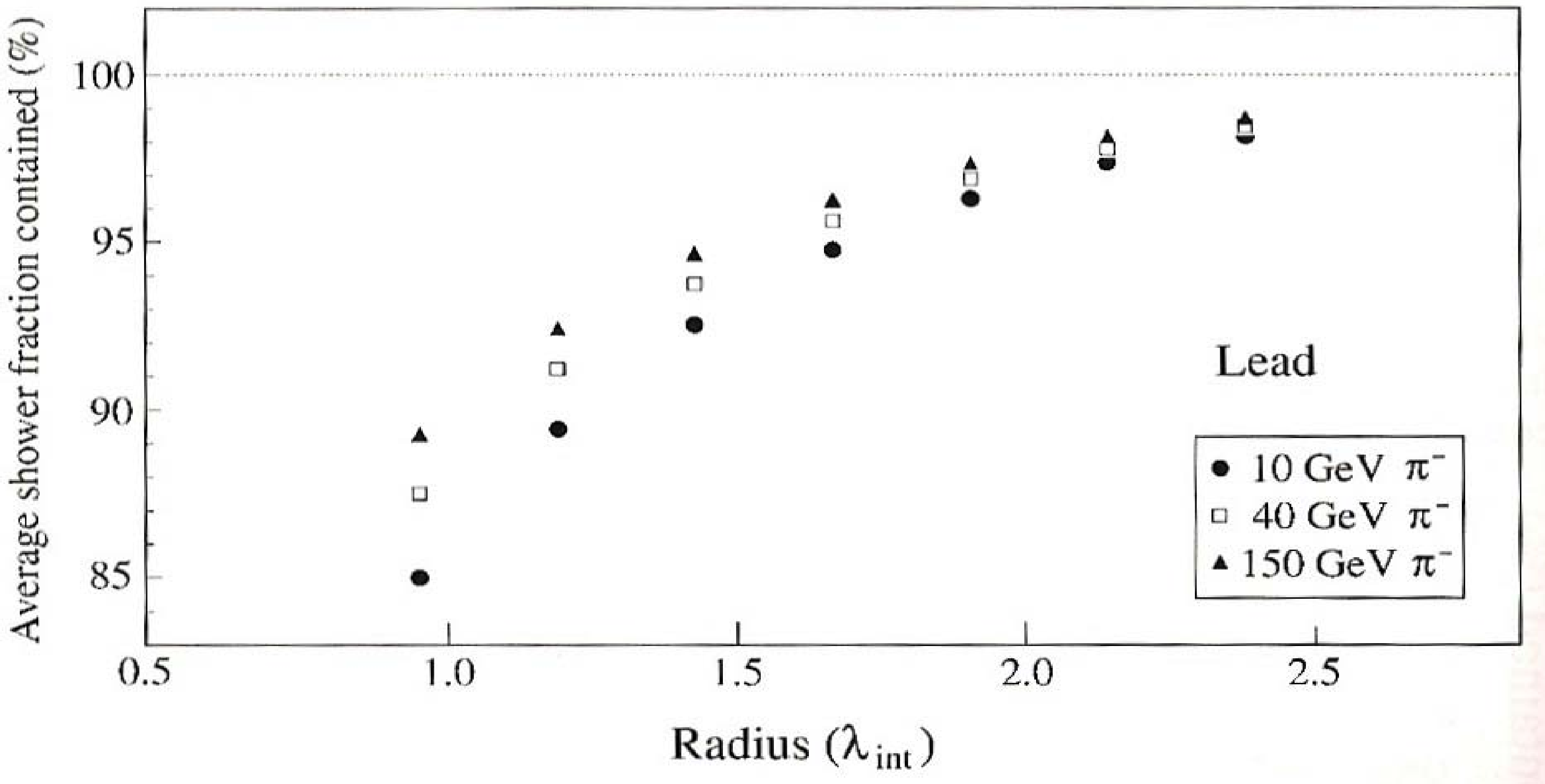

Average energy fraction contained in an infinitely long cylinder of absorber material, as function of the radius of this cylinder (expressed in λ_{int}) for pions of different energy showering in Pb.

II.4 Physics of Shower Development → Shower Particle Properties

- Electromagnetic component disappears after $\sim 5\ \lambda_{int}$

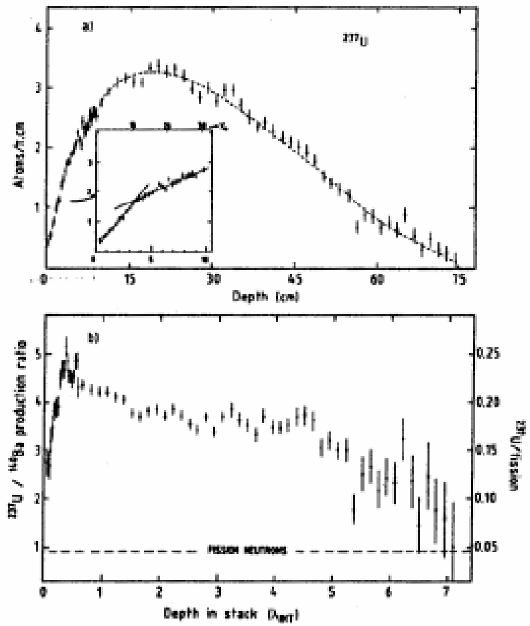

^{237}U produced by (γ, n), $(n, 2n)$,... reactions of ^{238}U
^{140}Ba produced by fission

Estimate : At $E_\pi = 300$ GeV $(58 \pm 7)\%$ of energy deposited by electromagnetic shower component

Source of electromagnetic component :
$\pi^0 \to \gamma\gamma,\quad \eta \to \gamma\gamma,\ \ldots$

Charge exchange : $\pi^- + p \to \pi^0 + n,\ \ldots$
$\pi^+ + n \to \pi^0 + p,\ \ldots$

Inverse reaction $\gamma + p \to \pi^+ + n,\ \ldots$

Negligible cross section : $\sigma(\gamma p) \approx \frac{1}{200}\,\sigma(\pi p)$

fraction f_{em} of energy deposited by electromagnetic shower increases with energy E_0 of primary particle

$$f_{em} = f_{\pi^0} \approx 0.1\ ln\ (E_0/1\ GeV)$$

II.4 Physics of Shower Development → Shower Particle Properties

Comparison of electromagnetic and hadronic shower :

Hadronic shower $\lambda_{int} = 35\ A^{1/3} g/cm^2$

Electromagnetic shower $X_0 \sim A/Z^2$ longitudinal

$R_M = \frac{21\ MeV}{\varepsilon_c}\ X_0$ transverse

Longitudinal width

$$\frac{\lambda_{int}}{X_0} \sim \frac{A^{1/3} Z^2}{A} \sim A^{4/3}$$

Transverse width

$$\frac{\lambda_{int}}{R_M} \sim \frac{A^{1/3} \cdot Z}{A} \sim A^{1/3}$$

II.4 Physics of Shower Development → Shower Particle Properties

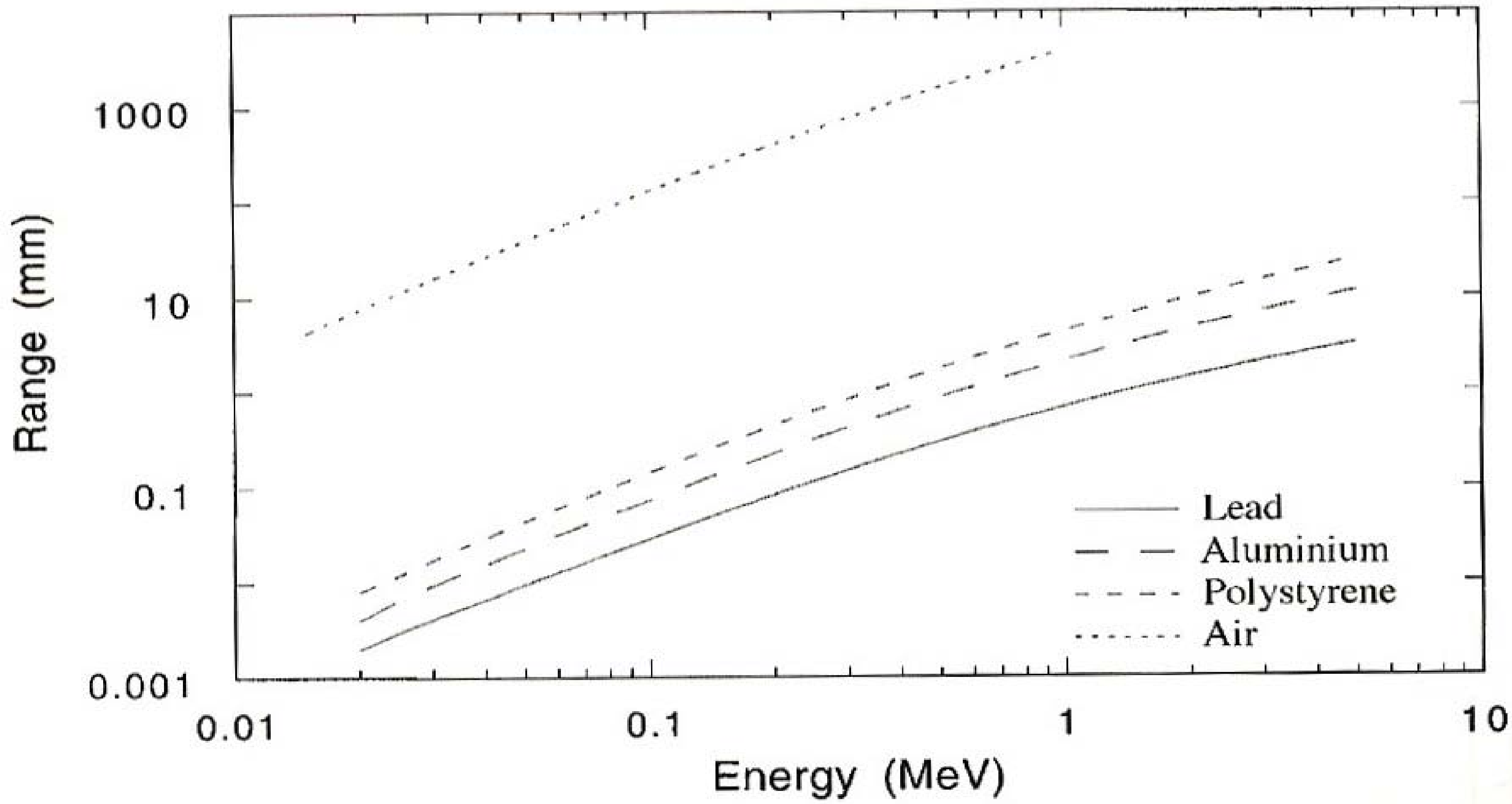

Average range of electrons in various absorber materials as function of energy.

II.4 Physics of Shower Development → Shower Particle Properties

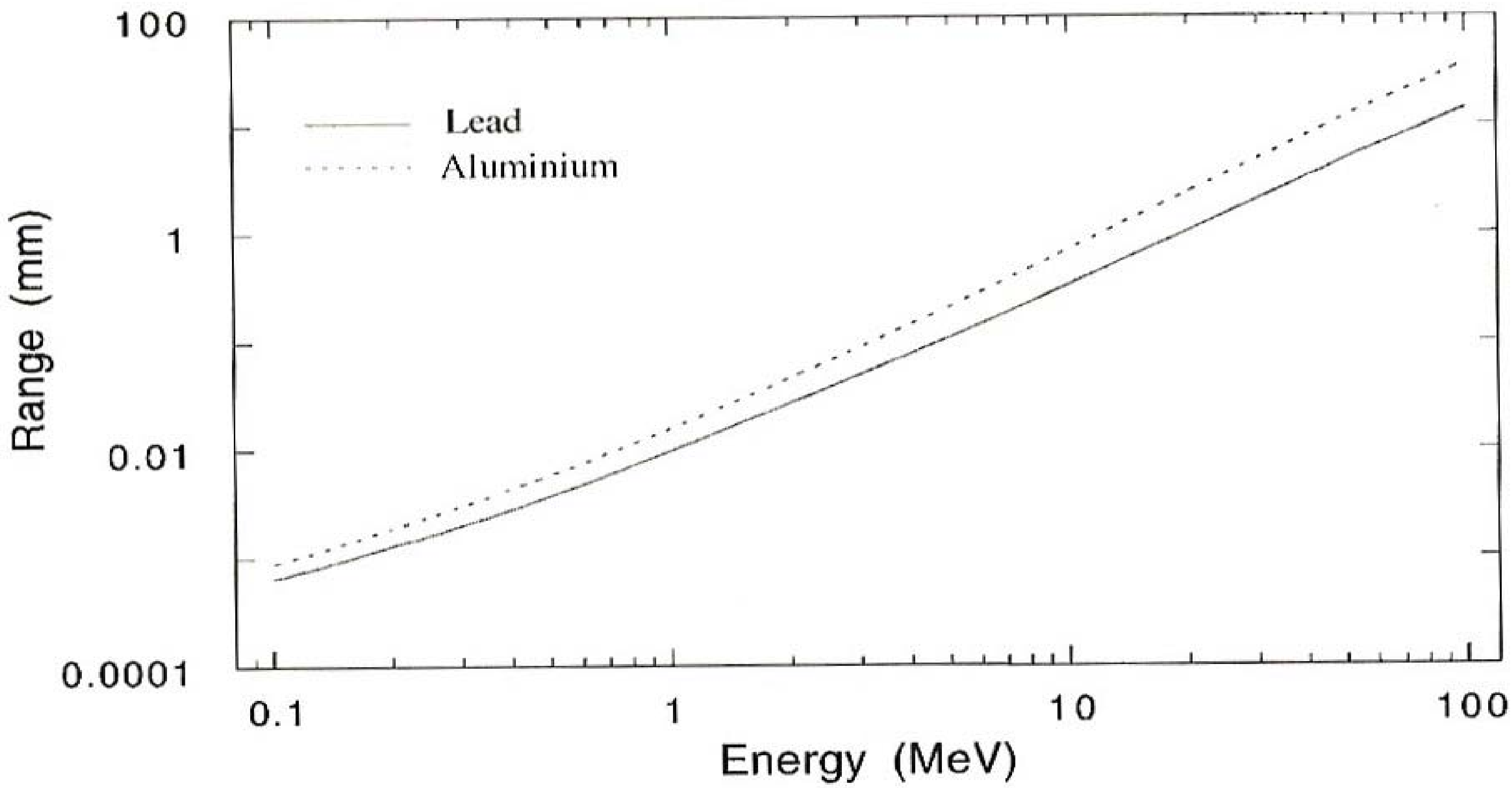

Average range of protons in various absorber materials as function of energy.

II.5 Physics of Shower Development → M.C. Simulations

1. **Electromagnetic showers**

   Detailed models exist (e.g. EGS4 code, GEANT)

2. **Hadron showers**

   - **Analytical models for hadron showers do not exist**
   - **MC models used to simulate showers**
   - **Many approximations necessary**
     - **Nuclear physics**
     - **Particle spectra produced**
     - **Neutron transport**
   - **Only approximate description of reality possible**
   - **Example code: GEANT4**
   - **Very time consuming calculations**
   - **Use parametrizations of energy depositions in shower (e.g. GFLASH)**

II.5.1 M.C. Simulations → Electromagnetic showers

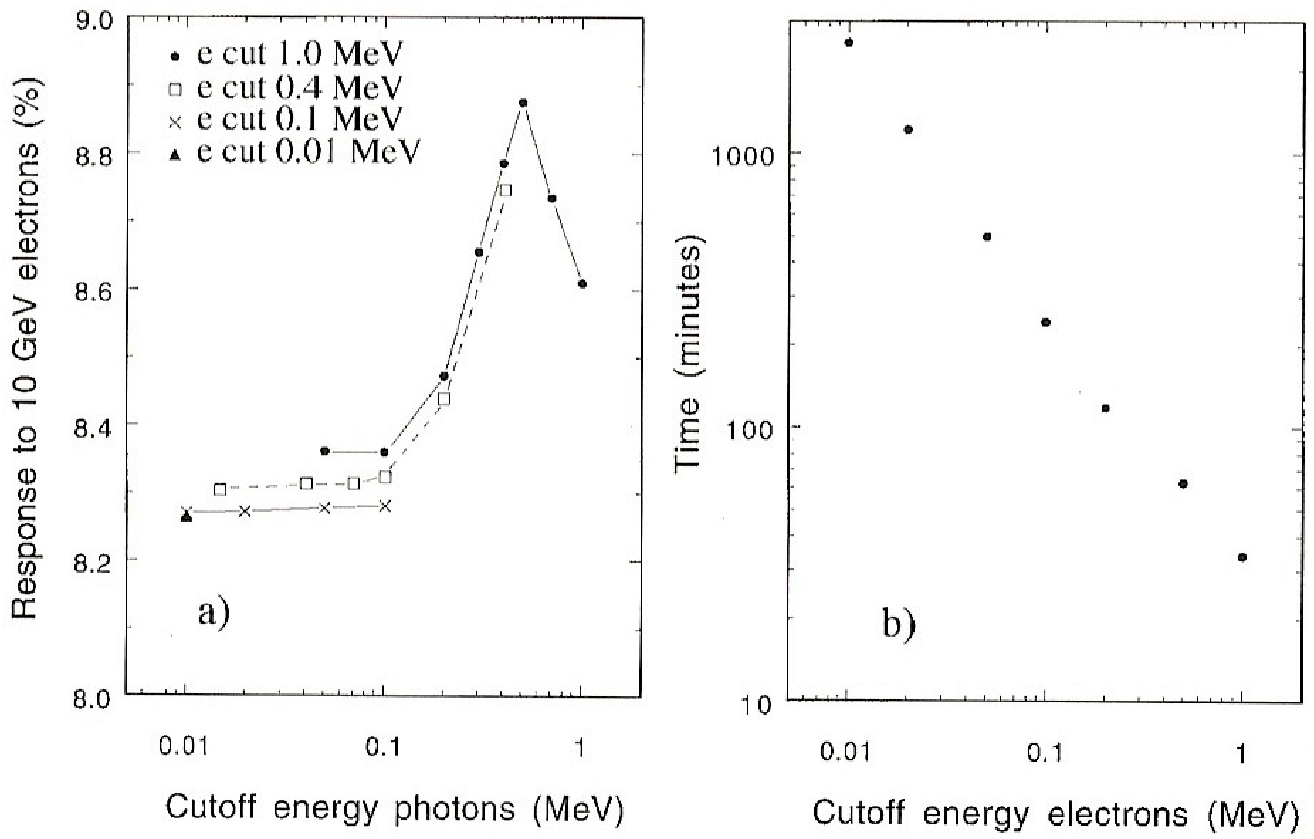

Effects of cut-off energy in EGS4 shower simulations. Shown are the average signals from 10 GeV electron showers in SPACAL.

a) Calculations for different values of the energy to which electrons and photons are tracked

b) Computer time needed for simulation of 1000 events as function of cut-off energy.

II.5.1 M.C. Simulations → Electromagnetic showers

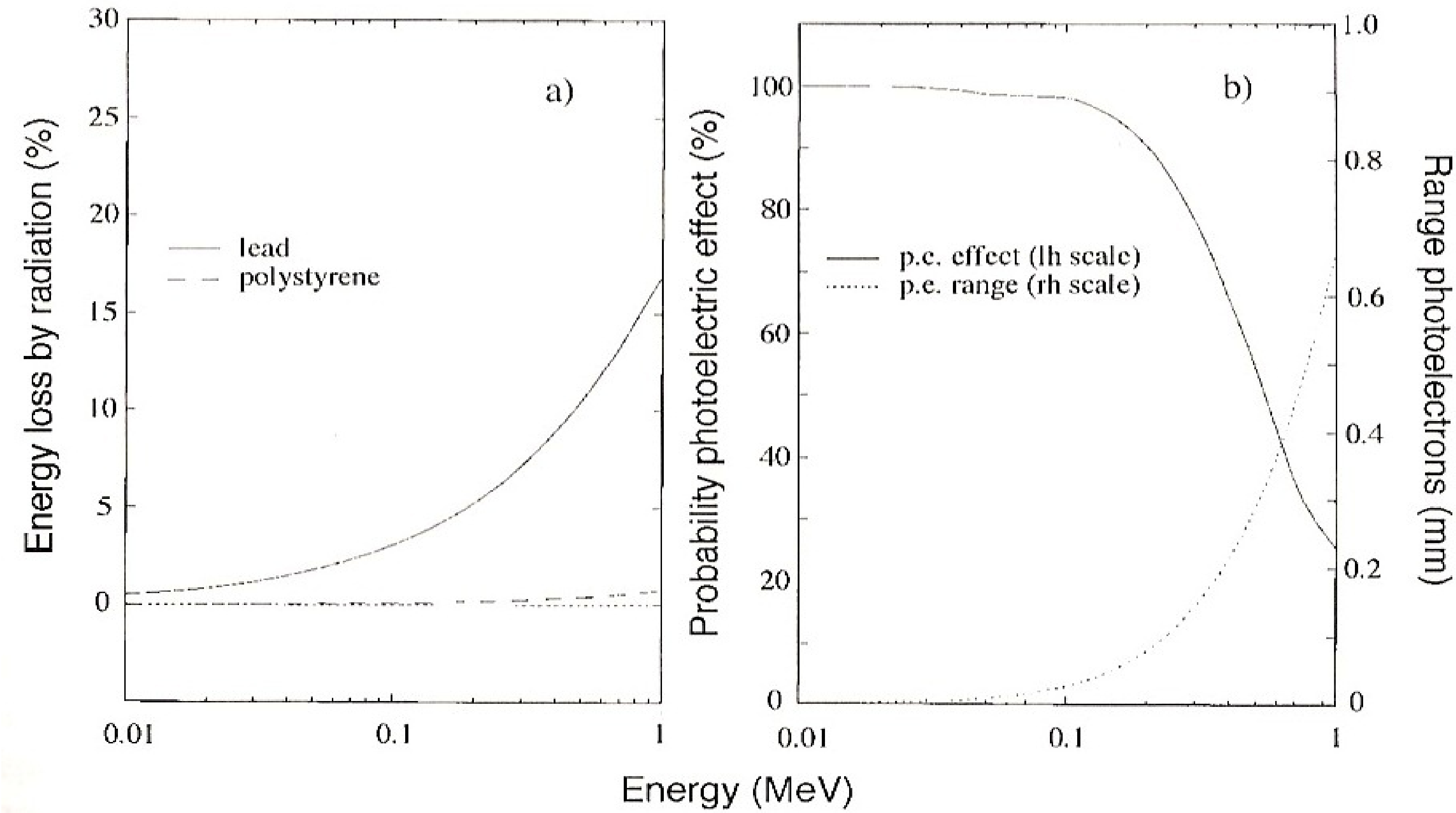

Energy fraction lost to bremsstrahlung by low-energy shower electrons in SPACAL.

a) Probability that low-energy photons interact through photoelectric effect in the absorber

b) Range of the photoelectrons produced as function of energy.